

AXISYMMETRIC FLOW PAST SLENDER BODIES

By

N. S. VENUGOPAL

TH
AE/1976/14
V569a

Thesis
629.132304
V569a



DEPARTMENT OF AERONAUTICAL ENGINEERING

INDIAN INSTITUTE OF TECHNOLOGY KANPUR

APRIL, 1976

AE
1976
M
VEN
AXT

AXISYMMETRIC FLOW PAST SLENDER BODIES

A Thesis Submitted
in partial Fulfilment of the Requirements
for the Degree of
MASTER OF TECHNOLOGY

By
N. S. VENUGOPAL

to the

DEPARTMENT OF AERONAUTICAL ENGINEERING
INDIAN INSTITUTE OF TECHNOLOGY KANPUR
APRIL, 1976

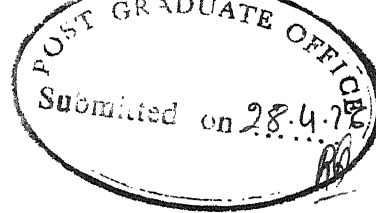


Theo's
622.132304
V5612

LIBRARY
CENTRAL
46310
Acc. No. A

AE-1976-M-VEN-AXI

29 MAY 1976



CERTIFICATE

This is to certify that the work "AXISYMMETRIC
TRANSONIC FLOW PAST SLENDER BODIES" has been
carried out under my supervision and has not been
submitted elsewhere for a degree.

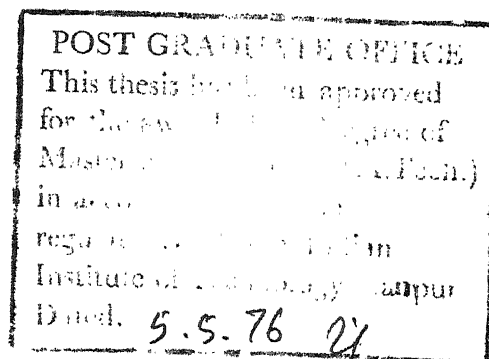
N.L. Arora

(N.L. ARORA)

Assistant Professor

Department of Aeronautical Engineering
Indian Institute of Technology, Kanpur

April 1976.



ACKNOWLEDGEMENTS

I express my sincere thanks to Dr. N. L. Arora for his guidance and advice.

I thank Mr. S. S. Pethkar for his neat and accurate typing and Mr. A.N. Upadhyaya for cyclostyling.

Finally, I express my thanks to my friends who helped me a lot at different stages of the work and during my stay at I.I.T. Kanpur.

April , 1976.

N.S. VENUGOPAL

TABLE OF CONTENTS

	Page
ABSTRACT	iii
LIST OF SYMBOLS	iv
LIST OF FIGURES	vii
 CHAPTER 1 INTRODUCTION	
1.1 General	1
1.2 Literature survey	3
1.3 Present work	10
 CHAPTER 2 PROBLEM FORMULATION	
2.1 Introduction	12
2.2 Basic equations and boundary conditions	14
2.3 Perturbation equations for axisymmetric flow	16
2.4 Normalization of transonic flow equations	22
 CHAPTER 3 INTEGRAL EQUATION APPROACH	
3.1 Introduction	24
3.2 Integral equation formulation	24
3.3 Simplification of integral equation	33
3.4 System of algebraic equations	35
3.5 Application of the method of parametric differentiation	36
 CHAPTER 4 LOCAL LINEARIZATION METHOD	
4.1 Introduction	39
4.2 Application of local linearization technique to axisymmetric flows	39
4.3 Fink's modification	46
4.4 Shock wave approximation	47
4.5 Method of solution	48

CHAPTER 5 COMPUTATIONAL DETAILS, RESULTS AND DISCUSSION

5.1	Introduction	51
5.2	Integral equation approach	51
5.2.1	Computational details	51
5.2.2	Results and discussion	53
5.3	Local linearization method	55
5.3.1	Computational details	55
5.3.2	Results and discussion	56
5.4	Conclusions	58
REFERENCES		60
APPENDIX A		62
APPENDIX B		64
APPENDIX C		
APPENDIX D		

ABSTRACT

In the present work the integral equation method has been applied to transonic axisymmetric flow. The governing differential equation for transonic axisymmetric flow is transformed into an integral equation using Green's theorem. Using functional relationship for velocity distribution, the double integral equation is reduced to an integral equation valid on the body surface. The integral equation is then converted into a set of algebraic equations. The method of parametric differentiation is then applied to these equations to get a system of first order nonlinear ordinary differential equations. These are solved using Hamming's predictor-corrector method upto the bifurcation point. Beyond the bifurcation point the steepest descent method is applied to the system of algebraic equations. In order to compare our results, the method of local linearization has also been studied in the process. The results are computed for a parabolic arc body of different fineness ratios at various Mach numbers by the integral equation approach and the local linearization method. The results obtained are compared with experimental results and the more accurate numerical results.

LIST OF SYMBOLS

a	-	speed of sound
C_p	-	Pressure coefficient
E	-	kernel function of the double integral defined by equation (3.27)
K	-	Transonic parameter
L	-	Laplacian operator
M	-	Mach number
n	-	normal to boundary surface
\bar{n}	-	Unit vector normal
N	-	Number of intervals
S	-	Boundary surface
\bar{u}	-	Perturbation velocity in \bar{x} -direction
\bar{u}_L	-	Linear perturbation velocity
\bar{v}	-	Perturbation velocity in \bar{r} direction
V	-	Volume bounded by the boundary surface
x, y, z	-	Cartesian coordinates
x, γ, θ	-	Cylindrical co-ordinates
$\bar{x}, \bar{\gamma}, \bar{\theta}$	-	Normalised cylindrical coordinates
γ	-	ratio of specific heats (= 1.4 for air)
ϵ	-	small non-dimensional parameter measuring the perturbation level
ξ, η, ζ	-	Running coordinates in $\bar{x}, \bar{y}, \bar{z}$ directions .

ξ, ρ, v	-	Running coordinate in $\bar{x}, \bar{r}, \bar{\theta}$ directions
μ	-	Artificial viscosity
τ	-	thickness ratio
ϕ	-	Perturbation velocity potential
$\bar{\phi}$	-	Normalised perturbation velocity potential
ψ	-	Parameter satisfying Laplace equation
ω	-	Solid angle
$< >$	-	Jump across the shock wave

Subscripts

cr	-	critical
D	-	shock discontinuity
i, j	-	values at different \bar{x} coordinates
P	-	singular point
x, y, z	-	Partial derivative of the variable with respect to x, y, z .
$\bar{x}, \bar{y}, \bar{z}$	-	Partial derivative of the variable with respect to $\bar{x}, \bar{y}, \bar{z}$.
ξ, η, ζ	-	Partial derivatives of the variable w.r.to the running coordinates ξ, η, ζ

∞	-	Free stream conditions
1	-	Conditions upstream of shock wave
2	-	Conditions downstream of shock wave

(1), (2)...- order of terms.

Superscripts

i - inner flow solution

o - outer flow solution

(1),(2)...- order of terms.

LIST OF FIGURES

1. Supersonic region and Mach lines for a parabolic arc of revolution in free air.
2. Body and coordinate system.
3. Region of integration.
4. Flow chart of the computer program for the integral equation approach.
5. Behaviour of influence coefficient.
6. Velocity distribution (Discontinuous case).
7. Comparison of pressure distribution (Continuous Case).
- 8-9. Comparison of pressure distribution (Discontinuous Case).
10. Pressure distribution for fineness ratio 10 at different Mach numbers.
11. Pressure distribution for fineness ratio 10 at various Mach numbers (Discontinuous Case).
12. Pressure distribution at $M_\infty = 0.800$ for different fineness ratios.
13. Pressure distribution at $M_\infty = 0.950$ for different fineness ratios.
14. Variation of function G with Mach number.
- 14a. Flow chart of the computer program for the local linearization method.
15. Comparison of pressure distribution (Continuous Case).

16. Comparison of Pressure distribution (discontinuous case).

17-18. Pressure distribution for fineness ratio 10 at high
transonic speeds by local linearization method.

CHAPTER 1

INTRODUCTION

1.1 GENERAL

The efforts of aeronautical research are focussed on the transonic range by the practical problem of flight in the transonic range and of flight vehicles passing through the speed of sound. There is a considerable difference in the flow pattern and the forces exerted on a moving body at transonic speeds and low subsonic speeds. Shock waves are an essential feature of transonic flow. The occurrence of shock on a moving body leads to a rapid increase in drag coefficient with increasing Mach number.

The term transonic flow designates flows in which the velocity in one region is subsonic while in the remaining region it is supersonic. The two regions are separated by sonic lines or sonic surfaces (see figure 1). In some cases shock wave is formed when the velocity exhibits a discontinuity at the boundary between two regions. In the lower transonic range when the free stream Mach number is slightly less than unity, there are one or more supersonic regions embedded in the subsonic flow while in the upper transonic range the supersonic flow encloses one or more subsonic flow regions. If the free stream Mach number is increased continuously from zero, the transonic range begins when the highest local Mach number reaches

unity and ends when the lowest local Mach number approaches unity.

The Prandtl-Glauert equation for the perturbation velocity potential for flow past slender configurations is

$$(1 - M_\infty^2) \phi_{xx} + \phi_{yy} + \phi_{zz} = 0 \quad (1.2.1)$$

Although equation (1.2.1) gave good results in the study of subsonic and supersonic flows it was found to be incapable of treating transonic flows. This failure is evidenced by the calculated value of ϕ_x growing to such magnitude that it can no longer be regarded as a small quantity when compared to U_∞ . In order to allow the study of transonic flow, terms upto second order were retained in the quasilinear partial differential equation for a steady flow of a perfect inviscid gas, from which equation (1.2.1) was derived. By doing so an equation of the form

$$(1 - M_\infty^2) \phi_{xx} + \phi_{yy} + \phi_{zz} = M_\infty^2 (\gamma + 1) \phi_x \phi_{xx} \quad (1.2.2)$$

is deduced. The above equation in cylindrical coordinates can be written as

$$[(1 - M_\infty^2) - M_\infty^2 (\gamma + 1) \phi_x] \phi_{xx} + \phi_{rr} + \frac{1}{r} \phi_r = 0 \quad (1.2.3)$$

which is the governing equation for axisymmetric transonic flow.

The coefficient for ϕ_{xx} in (1.2.3) makes the transonic equation both nonlinear and of mixed elliptic-hyperbolic type. If

this coefficient is positive, equation (1.2.3) is elliptic and represents locally subsonic flow; and if it is negative, equation (1.2.3) is hyperbolic and represents locally supersonic flow. The mixed character of the flow field may occur with local supersonic region embedded in a subsonic flow or with local subsonic regions embedded in a supersonic flow. From the basic assumptions of small disturbance theory it is found that the equation (1.2.3) is valid everywhere in the flow field, both fore and aft of the shock wave. At subsonic and supersonic speeds equation (1.2.3) is of the same order of accuracy as equation (1.2.1) although more difficult to solve because of its nonlinearity.

Cole and Messiter (1957) obtained equation (1.2.3) by systematic expansion procedure. They presented a system of equations for the first, second and higher approximations. By a similar procedure they obtained the boundary conditions on the axis of the body. An expression for the pressure coefficient and drag on the body is also derived.

1.2 LITERATURE SURVEY

The term $\phi_x \phi_{xx}$ in equation (1.2.3) introduces complications in its solution. Since no general mathematical theory exists for such equations, Aerodynamists had to develop their own methods, for its solution. Many methods have been used to treat two-dimensional transonic flow using equation (1.2.2) such as analytical hodograph

methods, relaxation methods and Oswatitsch's integral equation method. For the transonic flow around smooth bodies of revolution the integral equation method would suit very well but attempts with this method are quite disappointing.

Oswatitsch and Keune (1955) introduced the parabolic method. They proposed that the transonic flow equation could be approximated for flows with $M_\infty = 1$, past slender bodies of revolution, by replacing $\phi_x \phi_{xx}$ by $K \phi_x$ where K is the acceleration parameter, a constant. The resulting equation is linear parabolic and has the form of equation of heat conduction. Accuracy of the above method depends on the value of acceleration parameter, K . To solve the parabolic equation a characteristic method was developed and the value of K which best fits the results of the characteristic method is taken. Although the parabolic method is direct and simple in application, the results lack accuracy. The predicted flow is in good agreement with the data for forebodies where the assumption is valid. Poor agreement occurs for the aft part where the axial velocity gradient is constant and negative.

Maeder and Thommen (1956) observed that the assumption made by Oswatitsch and Keune (1955) is not close to the actual behaviour of the fluid at all speeds than originally suspected. They suggested that the value of K should be determined at the point of maximum velocity in the incompressible case. The results obtained by them are in fair agreement with the experimental ones.

Heaslet and Spreiter (1956) applied the integral equation method to transonic flow around slender wings and bodies of revolution. Special attention was given to conditions resulting from shock waves and to the reduction of relations to special forms necessary for discussion of the sonic flow with $M_\infty = 1$. Results obtained for cone-cylinders, wings and wing body combinations at a free stream Mach number 1 were seen to be in good agreement with experimental results. An example has also been given in which the general result is applied to calculate pressure and integrated forces on a family of slender, elliptic cone-cylinders.

Spreiter and Alksne (1959) introduced the so called local linearization method, which grew out of the parabolic method of Oswatitsch and Keune (1956). The idea is to linearize the nonlinear transonic flow equation by replacing either ϕ_{xx} or ϕ_x in the nonlinear term by a constant λ , solving the simplified equation, and then introducing different values for λ for different points in the flow. This procedure can be considered as equivalent in some sense to replacing the original nonlinear partial differential equation at each point. Results obtained by such a procedure depend on the choice of λ and must be assembled to determine the final results. This step is accomplished by putting the results into such a form that a first order nonlinear ordinary differential equation is obtained for the streamwise perturbation velocity component $u = \phi_x$, after λ is replaced by the quantity it originally represented. In many cases,

this equation is of sufficiently simple form that it can be integrated analytically and the solution expressed in closed form. In other cases, the integration must be done numerically, but the equation is of such a form that standard methods can be applied. Spreiter and Alksne (1959) applied this method to planar flow past thin airfoils and flow past slender bodies of revolution and obtained useful results. Of all the approximate methods presently available this has been the most versatile and of consistent accuracy comparable with theoretical and experimental results.

Hosokawa (1959, 1962) observed that the parabolic method of Oswatitsch and Keune (1956) and later extended by Maeder and Thommen (1956) had two drawbacks. Firstly it is seen that the calculated flow is not influenced by the mixed flow character and the movement of the sonic point with increasing Mach number is given incorrectly. He proposed a refinement of the method to remove such defects. The basic concept of the method of Hosokawa is that the solution for $u = \phi_x$ is considered to be written in the form

$$u = \tilde{u} + g_x \quad (1.2.4)$$

where g_x is the correction factor and $\tilde{u} = \bar{\phi}_x$ satisfies

$$(1 - M_\infty^2) \bar{\phi}_{xx} + \bar{\phi}_{yy} + \bar{\phi}_{zz} = K \bar{\phi}_x \quad (1.2.5)$$

An approximate equation is obtained for g_x with the use of (1.2.4)

and (1.2.5). Hosokawa suggested that the constant K should be determined so that the solution of equation (1.2.5) should be a good approximation in the vicinity of the sonic point on the body surface. Thus the sonic point and the value of K is simultaneously determined. The occurrence of shock is also predicted and is seen that it is closer to the experimental data. Maeder and Thommen (1961) pointed out that Hosokawa's method is not appropriate where the flow acceleration at the sonic point is large. A detached shock wave appearing upstream of the body when $M_\infty \gtrsim 1$, and sonic freezing of the flow cannot be derived by this method.

Sandeman (1962) applied the local linearization technique to solve the choked wind tunnel flow problems. By the use of local linearization method and suitable adjustment of the scale of the transonic asymptotic solution used to represent the tunnel wall pressure distribution, the correction can be made of the same order of magnitude as that given by the more reliable results of transonic theory over a useful range of profile to wind tunnel dimensions. The use of the method for axisymmetric flows has added difficulties and there appear to be no more reliable theoretical corrections available for comparison with the result of these methods.

Spreiter and Stahara (1970,1971) combined local linearization method with transonic equivalence rule for studying three dimensional flows. They developed programs for three dimensional axisymmetric transonic flows about bodies of revolution to determine

surface and flow field pressure distributions. Programs are also developed to calculate the lower critical Mach number and upper critical Mach number. Comparisons of results predicted by the above programs show for the axisymmetric bodies studied, the predicted surface and flow field pressure distributions are in essential agreement over the fore part of the bodies and diverge near the rear part. This discrepancy is attributed to the shock wave boundary layer interaction and wind tunnel wall interference effects. Results also indicate that the order of magnitude of disturbances are smaller in the axisymmetric case than the two-dimensional case.

Fink (1971) observed that the local linearization technique for transonic flow past slender axisymmetric bodies gave good results at Mach numbers close to one and poor agreement at other transonic speeds. He suggested some changes in local linearization technique to provide reasonable predictions near the high and low ends of the transonic regime while retaining the previous good agreement at near-sonic speeds. A revision of Spreiter and Alksne's (1959) solution for accelerating, locally near-sonic flow and an empirical description of shock wave strength and location are patched to the local linearization equations for locally subsonic and supersonic flows. Calculated pressure distributions are in good agreement with experimental data.

During the past few years some numerical methods have been developed to predict inviscid transonic flows, including embedded

shocks about two dimensional airfoils and slender bodies of revolution. The most efficient techniques at present use relaxation methods to solve finite difference approximations to the governing steady state equations. Bailey (1971) described a relaxation method for the numerical solution of the small disturbance equation for flow past a slender body of revolution. His results for subcritical flows agree well in the region near the forward portion of the body. The computed values for supercritical flow showed slightly more negative C_p as well as a shock location slightly upstream of the experimental location.

Krupp and Murman (1972) developed a numerical method to solve the transonic flow equation in application to two-dimensional and axisymmetric flows. A difference scheme is used to represent the derivatives. An analytic expression derived for the far field by Guderley (1950) is used as an outer boundary condition. The difference equations are solved by a line relaxation algorithm. Results obtained for $M_\infty < 1$, including cases with shock waves for airfoils and slender bodies of revolution showed good agreement with experimental data.

Recently Sedin (1975) described a method for calculating axisymmetric sonic flow, which is an extension of the work done by Sedin and Berndt (1970). The idea is to generalise slender body behaviour close to the body to decompose the velocity potential into two new functions. A differential system of two coupled

equations is then formed. If the equations for the two new functions are regarded one at a time, assuming the other function to be known, the system can be temporarily interpreted as two parabolic equations. The time like variables for the two equations are then defined in two opposite directions. Then the two equations are integrated alternatively, using the boundary/condition as initial values for one of the functions and the Guderley (1950) far field expansion as initial data for the other function. This technique has been found to be a fast and reliable tool for computing axisymmetric sonic flow. The rate of convergence is high. The agreement with experimental data and other methods of computation is found to be very good.

1.3 PRESENT WORK

Much work has been done in the case of two-dimensional flows rather than the axisymmetric case. The integral equation method applied to two dimensional flows has proved to give good results. However, the attempts to solve the problem of mixed transonic flow past slender bodies of revolution by the integral equation method have been disappointing. The local linearization technique still remains a powerful tool in obtaining approximate solution to the transonic flow equation for the axisymmetric case. The local linearization technique as applied today can at best be described as an engineering approximation to obtain the solution to the transonic flow problems.

In order to fill the gap an attempt has been made here to solve the problem of mixed transonic axisymmetric flow, using the integral equation approach. In order to compare our results, in the process, the local linearization technique has also been studied. In Chapter 2 the governing equations and boundary conditions have been deduced with the help of asymptotic matching principle. In Chapter 3 the integral equation method has been applied to the axisymmetric case and the integral equation is converted into a set of algebraic equations. The solution to the set of algebraic equations is obtained by the method of parametric differentiation. Chapter 4 deals with the local linearization technique for axisymmetric flow problem. Finally in Chapter 5 the computational details has been given. The results are computed for a parabolic arc body of different fineness ratios and at different Mach numbers. The discussion and the conclusions drawn are finally presented.

CHAPTER 2

PROBLEM FORMULATION

2.1 INTRODUCTION

The transonic flow over slender bodies, in general, involve curved shocks over the body surface. When the upstream Mach number is not far from sonic, the vorticity, as well as the variation in entropy, produced in the downstream flow due to the curved shocks may be ignored for all practical purposes. Consequently the entire flow may be considered isoenergetic, homentropic and irrotational despite the presence of shocks and it is then possible to define a velocity potential.

The small perturbation theory for subsonic and supersonic flow breaks down at transonic speeds. This becomes evident from the linearized differential equation for the perturbation potential, which in the limit $M_\infty \rightarrow 1$ becomes

$$\frac{1}{r} \phi_r + \phi_{rr} = 0$$

for axisymmetric flow. Thus it will not be possible to satisfy the boundary condition of vanishing disturbance at infinity. This failure corresponds to a nonuniformity in the expansion procedure. It is implicit in the linearized theory that the dimensionless velocity perturbations in x and r directions

ϕ_{1x}, ϕ_{1r} are of the same order of magnitude. On the other hand an examination of the exact solution of simple supersonic flow like expansion around a corner, [see e.g. Liepmann and Roshko (1956)] shows that the perturbations in x and r directions (u, v) from a uniform sonic stream in the x -direction are related as $v \sim u^{3/2}$. A similar result holds for weak oblique shock waves in the transonic range. This sort of order of magnitude relation will be required, in the large, for the perturbations of the basic transonic approximation. If it is known that a potential exists (as is the case) this last requirement has interesting consequence that expansion must be carried out in a distorted set of coordinates. For example represent the perturbation potential by $\epsilon \phi_1(x, \rho)$ where $\rho = \epsilon^{\frac{1}{2}} r$, so that the actual velocity perturbations $\frac{\partial}{\partial x}(\epsilon \phi_1)$, $\frac{\partial}{\partial r}(\epsilon \phi_1)$ are of correct order of magnitude. An interpretation of this coordinate ρ is given by saying that in the transonic range, perturbations carried by a body in the flow extends much farther in the transverse direction (large r) than in the flow direction and that a reduced coordinate ρ must be used to bring these disturbances back in view. All these physical considerations are the basis for more general form of expansion which must be used in the transonic case. The expansion procedure for axisymmetric flow has been carried out by Cole and Messiter (1957).

In section 2.2 the basic equations and the boundary conditions for axisymmetric flow past bodies of revolution

have been discussed. In section 2.3 transonic flow equation for perturbation potential and consistent boundary conditions have been derived by using the asymptotic matching principle [see e.g. Ashley and Landahl 1965]. The expression for the pressure coefficient C_p is given and a small disturbance approximation to the shock jump conditions have been obtained. In section 2.4 the equations obtained in the previous section have been normalized using suitable transformations for subsonic Mach numbers.

2.2 BASIC EQUATIONS AND BOUNDARY CONDITIONS

We shall consider the flow around a slender nonlifting body of revolution defined by

$$r = R(x) = \tau \bar{R}(x) \quad (2.1)$$

for small values of thickness ratio τ . The body axis is aligned with the free stream direction.

For axisymmetric flow, using the conservation equations for compressible, inviscid and nonheat conducting potential flow of a perfect gas, the differential equation for velocity potential ϕ reads [see e.g. Ashley and Landahl (1965)] ,

$$(a^2 - \phi_x^2) \phi_{xx} + (a^2 - \phi_r^2) \phi_{rr} + \frac{a^2}{r} \phi_r - 2\phi_x \phi_r \phi_{xr} = 0 \quad (2.2)$$

where a is the sonic velocity defined by

$$a^2 = a_\infty^2 - \frac{\gamma-1}{2} (\phi_x^2 + \phi_r^2 - U_\infty^2), \quad (2.3)$$

Here U_∞ and a_∞ represent the free stream values of the flow velocity and the velocity of sound.

Shock waves are a prominent feature of transonic flows: Hence additional relations are needed for the transition through the shock. ϕ is continuous across the shock wave, while the axial and radial component of velocities (u, v) are discontinuous. The velocity components across the shock are related by the shock polar equation [see e.g. Cole and Messiter (1957)]

$$v^2 = (\tilde{u}_1 - \tilde{u}_2) \frac{\tilde{u}_1 \tilde{u}_2 - \frac{\gamma-1}{\gamma+1} \tilde{u}_1^2 - \frac{2}{\gamma+1} a_1^2}{\tilde{u}_1^2 - \tilde{u}_1 \tilde{u}_2 + \frac{2}{\gamma+1} a_1^2} \quad (2.4)$$

where subscripts 1 and 2 denote the conditions immediately ahead of and behind the shock. a_1 is the sonic velocity ahead of the shock and is given by

$$a_1^2 = a_\infty^2 - \frac{\gamma-1}{2} [\tilde{u}_1^2 + \tilde{v}_1^2 - U_\infty^2] \quad (2.5)$$

The boundary condition to be applied at the body surface is one of tangent flow at the surface. Hence,

$$\frac{\phi_r}{\phi_x} = \tau \frac{d\bar{R}}{dx} \quad \text{at } r = \tau \bar{R}(x) \quad (2.6)$$

The other boundary condition is that all flow disturbances die out at upstream infinity.

The local pressure coefficient can be obtained from [see e.g. Liepmann & Roshko (1965)]

$$C_p = \frac{2}{\gamma M_\infty^2} \left\{ \left[1 - \frac{\gamma-1}{2a_\infty^2} (\phi_x^2 + \phi_r^2 - U_\infty^2) \right]^{\frac{\gamma}{\gamma-1}} - 1 \right\} \quad (2.7)$$

For small flow disturbances equation (2.7) can be simplified to obtain

$$C_p = - \frac{\phi_x^2 + \phi_r^2 - U_\infty^2}{U_\infty^2} + \frac{M_\infty^2}{4} \left(\frac{\phi_x^2 + \phi_r^2 - U_\infty^2}{U_\infty^2} \right)^2 + \dots \quad (2.8)$$

2.3 PERTURBATION EQUATIONS FOR AXISYMMETRIC FLOW

We seek first an outer expansion of the form

$$\phi = U_\infty [x + \varepsilon \phi_1^0(x, \rho) + \varepsilon^2 \phi_2^0(x, \rho) + \dots] \quad (2.9)$$

where ε is a small nondimensional parameter measuring the perturbation level and

$$\rho = \delta r \quad (2.10)$$

with δ being a function of ε so that

$$\delta \rightarrow 0 \quad \text{as} \quad \varepsilon \rightarrow 0.$$

By introducing the expansion (2.9) into (2.3) and (2.4), we obtain

after neglecting higher order terms in ϵ or δ

$$[(1 - M_\infty^2) - \epsilon(\gamma+1) M_\infty^2] \phi_{1x}^0 + \delta^2 \left[\frac{1}{\rho} \phi_{1\rho}^0 + \phi_{1\rho\rho}^0 \right] = 0 \quad (2.11)$$

Here $(1 - M_\infty^2) \sim O(\epsilon)$. Thus comparing order of magnitude of each term in (2.11), it is noted that non-degenerate equation is obtained by setting

$$\delta^2 \sim \epsilon \quad (2.12)$$

Let us select $\delta = M_\infty \sqrt{\epsilon(\gamma+1)}$. Equation (2.11) then becomes

$$-(K + \phi_{1x}^0) \phi_{1xx}^0 + \frac{1}{\rho} \phi_{1\rho}^0 + \phi_{1\rho\rho}^0 = 0 \quad (2.13)$$

$$\text{where } K = \frac{M_\infty^2 - 1}{\epsilon(\gamma+1) M_\infty^2} \quad (2.14)$$

K is called the transonic parameter. Equation (2.13) is basically nonlinear and Mach number enters through the transonic parameter K .

The only boundary condition available for equation (2.13) so far is that flow perturbations must vanish at large distances, i.e.

$$\phi_{1x}^0, \phi_{1\rho}^0 \rightarrow 0 \quad \text{as } x, r \rightarrow \infty \quad (2.15)$$

The remaining boundary condition belongs to the inner region and is to be obtained by matching of the inner and outer flow solutions.

The inner flow expansion is sought in the form

$$\phi^i = U_\infty [x + \epsilon \phi_1^i(x, r) + \epsilon^2 \phi_2^i(x, r) + \dots] \quad (2.16)$$

Using expansion (2.16) into (2.2), (2.3) and (2.6) we find that the inner flow is governed by

$$\left. \begin{aligned} \phi_{1rr}^i + \frac{1}{r} \phi_{1r}^i &= 0 \\ \epsilon \phi_{1r}^i(x, R) &= \frac{dR}{dx} = \tau \frac{d\bar{R}}{dx} \end{aligned} \right] \quad (2.17)$$

with the solution

$$\begin{aligned} \epsilon \phi_1^i(x, r) &= \frac{1}{2\pi} S'(x) \ln r + g_1(x) \\ &= \tau^2 \left[\frac{1}{2\pi} \bar{S}'(x) \ln r + \bar{g}_1(x) \right] \end{aligned} \quad (2.18)$$

The inner solution cannot, of course, give vanishing disturbances at infinity since this boundary condition belongs to the outer region. We therefore need to match the inner and outer flow solutions. For this we shall use the asymptotic matching principle.

The inner solution (2.18) gives,

$$\begin{aligned} \epsilon \phi_{1r}^i(x, r) &= \frac{\tau^2}{2\pi} \frac{\bar{S}'(x)}{r} \\ \text{so that, } r \phi_{1r}^i &= \frac{1}{2\pi} \frac{\tau^2}{\epsilon} \bar{S}'(x) \end{aligned} \quad (2.19)$$

Since $\rho = \delta r$, by application of the limit matching principle to the radial velocity component, with the choice,

$$\epsilon = \tau^2$$

we find

$$\lim_{\rho \rightarrow 0} [\rho \phi_{1\rho}^0] = \frac{1}{2\pi} \bar{S}'(x) = \frac{1}{2\pi} S'(x) \quad (2.20)$$

the boundary condition for the outer flow.

The perturbation velocity potential in case of a slender axisymmetric body is thus of order τ^2 , as compared to $\tau^{2/3}$ for the two dimensional case [see Ashley and Landahl (1965)]. Since the disturbances are of, at least, an order of magnitude smaller in the axisymmetric case for a given thickness ratio, one would expect the transonic region to be correspondingly smaller than in two-dimensional case.

Introducing the outer expansion (2.9) for ϕ in the expression for C_p , Eqn. 2.8, and neglecting the terms of order ϵ^3 and higher we get,

$$C_p = -2\epsilon \phi_{1x}^0 - \epsilon^2 \phi_{1r}^0{}^2 - \epsilon^2 \phi_{1x}^2 \quad (2.21)$$

If, now one defines the perturbation velocity potential for outer flow as

$$\phi = \epsilon \phi_1^0$$

and return to original coordinates (x, r) the following formulation of transonic axisymmetric flow problem is obtained.

$$[1 - M_\infty^2 - (\gamma + 1) M_\infty^2 \phi_x] \phi_{xx} + \frac{1}{r} \phi_r + \phi_{rr} = 0 \quad (2.22)$$

with the boundary conditions

$$\left. \begin{aligned} \lim_{r \rightarrow 0} (r \phi_r) &= R \frac{dR}{dx} \\ &= \frac{S'(x)}{2\pi} \\ \phi_r, \phi_x &\rightarrow 0 \text{ at infinity} \end{aligned} \right] \quad (2.23)$$

The pressure coefficient is given by

$$C_p = -2\phi_x - \phi_r^2 \quad (2.24)$$

which on the body surface $r = R(x)$ becomes

$$C_p = -2u - \left(\frac{dR}{dx} \right)^2 \quad (2.24a)$$

The shock jump conditions can be obtained using the expansions assumed for perturbation velocity potential ϕ [equation (2.9)] in equation (2.4). Hence we write the expansions for velocities as

$$\left. \begin{aligned} \frac{u}{U_\infty} &= 1 + \epsilon u^{(1)} + \epsilon^2 u^{(2)} + \dots \\ \frac{v}{U_\infty} &= \epsilon^{3/2} [v^{(1)} + \epsilon v^{(2)} + \dots] \end{aligned} \right] \quad (2.25)$$

Substituting (2.25) in the shock polar equation (2.4) one obtains

$$\begin{aligned} \epsilon^3 U_\infty^3 v_2^{(1)2} \left[\frac{2}{\gamma+1} \frac{1}{M_\infty^2} + \epsilon(u_1^{(1)} - u_2^{(1)}) - 2\epsilon \frac{\gamma-1}{\gamma+1} u_1^{(1)} + O(\epsilon^2) \right] = \\ \epsilon^3 U_\infty^3 (u_1^{(1)} - u_2^{(1)})^2 \left[-\frac{2}{\gamma+1} \frac{1-M_\infty^2}{M_\infty^2} + \epsilon(u_1^{(1)} + u_2^{(1)}) + O(\epsilon^2) \right] \end{aligned} \quad (2.26)$$

Equating the coefficients of terms of $O(\epsilon^3)$ in (2.26), we obtain first approximation for the shock polar as

$$[u_2^{(1)} - u_1^{(1)}] [(1 - M_\infty^2)(u_2^{(1)} - u_1^{(1)}) - (\gamma + 1)M_\infty^2 \frac{u_2^{(1)2} - u_1^{(1)2}}{2}] + v_2^{(1)2} = 0 \quad (2.27)$$

Equation (2.27) can also be written as

$$[(1 - M_\infty^2) \langle u \rangle - \frac{\gamma + 1}{2} M_\infty^2 \langle u^2 \rangle] \langle u \rangle + \langle v \rangle^2 = 0 \quad (2.28)$$

where $\langle u \rangle = u_2 - u_1$

$$\langle v \rangle = v_2 - v_1.$$

This may be regarded as a small disturbance approximation to the shock jump conditions.

From the irrotationality condition, for flow ahead of the shock we can write

$$\iiint_V \frac{\partial u_1}{\partial x} dV = \iiint_V \frac{\partial v_1}{\partial x} dV$$

which by the use of divergence theorem yields

$$\iint_S u_1 n_2 dS = \iint_S v_1 n_1 dS \quad (2.29)$$

Similarly for the other side of the shock, we have

$$\iint_S u_2 n_2 dS = \iint_S v_2 n_1 dS \quad (2.30)$$

Subtracting (2.30) from (2.29), we obtain

$$\iint_S [\langle u \rangle n_2 - \langle V \rangle n_1] dS = 0 \quad (2.31)$$

Since S is any arbitrary chosen surface, we can write from (2.31)

$$\langle u \rangle n_2 - \langle V \rangle n_1 = 0$$

$$\text{i.e.} \quad \langle u \rangle \cos \theta_2 - \langle V \rangle \cos \theta_1 = 0 \quad (2.32)$$

Relation (2.32) combined with equation (2.28) gives

$$\{ (1 - M_\infty^2) \langle u \rangle - \frac{\gamma+1}{2} M_\infty^2 \langle u^2 \rangle \} \cos \theta_1 + \langle v \rangle \cos \theta_2 = 0 \quad (2.33)$$

a second form of the shock jump condition for weak jumps.

2.4 NORMALIZATION OF TRANSONIC FLOW EQUATIONS

For subsonic free stream Mach numbers, it is convenient to introduce the following transformations

$$\left. \begin{aligned} \bar{x} &= x \\ \bar{r} &= r(1 - M_\infty^2)^{\frac{1}{2}} \\ \bar{\phi} &= \frac{(\gamma+1)M_\infty^2}{1 - M_\infty^2} \phi \end{aligned} \right\} \quad (2.34)$$

Then the transonic equation (2.22) for axisymmetric flows can be expressed as

$$\bar{\phi} \frac{\partial^2}{\partial \bar{x}^2} + \bar{\phi} \frac{\partial^2}{\partial \bar{r}^2} + \frac{1}{\bar{r}} \frac{\partial \bar{\phi}}{\partial \bar{r}} = \bar{\phi} \frac{\partial^2}{\partial \bar{x}^2} \frac{\partial^2}{\partial \bar{x}^2} \quad (2.35)$$

The boundary conditions (2.23) then reduce to

$$\left. \begin{aligned} \lim_{\bar{r} \rightarrow 0} (\bar{r} \bar{\phi}_{\bar{r}}) &= \frac{(\gamma+1) M_{\infty}^2}{(1-M_{\infty}^2)} \frac{S'(x)}{2\pi} \\ \bar{\phi}_{\bar{x}}, \bar{\phi}_{\bar{r}} &\rightarrow 0 \text{ at infinity} \end{aligned} \right] \quad (2.36)$$

and the shock condition (2.28) or (2.33) becomes

$$[\langle \bar{u} \rangle \frac{1}{2} \langle \bar{u}^2 \rangle] \langle \bar{u} \rangle + \langle \bar{v} \rangle^2 = 0 \quad (2.37)$$

or

$$[\langle \bar{u} \rangle - \langle \bar{u}^2 \rangle] \cos \theta_1 + \langle \bar{v} \rangle \cos \theta_2 = 0 \quad (2.38)$$

The relation (2.24 a) for pressure coefficient gives on the body surface

$$C_p = \frac{-2(1-M_{\infty}^2)}{(\gamma+1) M_{\infty}^2} \bar{\phi}_{\bar{x}} - \left(\frac{d\bar{R}}{d\bar{x}} \right)^2 \quad (2.39)$$

CHAPTER 3

INTEGRAL EQUATION APPROACH

3.1 INTRODUCTION

In this chapter the governing nonlinear partial differential equation of transonic flow is transformed into an integral equation using Green's theorem for supercritical speeds [$M_\infty < 1$; $M_{cr} < M_\infty$]. The integral equation in cylindrical coordinates is simplified using a functional relationship for velocity perturbation. This gives an integral equation on the body surface. The equation so obtained is converted into a set of nonlinear algebraic equations using Gauss Quadrature.

The solution to these equations can be obtained through iterative schemes. However difficulty arises due to the fact that it admits multivalued discontinuous solutions. Hence to control the development of an iterative solution to the system, the method of parametric differentiation is used; the parameter introduced is the so called artificial viscosity. The method is similar to the one used by Norstrud (1973) for the treatment of two-dimensional symmetric airfoils.

3.2 INTEGRAL EQUATION FORMULATION APPLICATION OF GREEN'S THEOREM

We apply Green's theorem to equation (2.35), which relates surface integral to volume integral. The theorem states that the

following relation holds between any two arbitrary functions of $\bar{\phi}$ and ψ having continuous first and second derivatives in the volume V bounded by the surface S

$$\iiint_V [\psi L(\bar{\phi}) - \bar{\phi} L(\psi)] dV = \iint_S \left(\bar{\phi} \frac{\partial \psi}{\partial n} - \psi \frac{\partial \bar{\phi}}{\partial n} \right) dS \quad (3.1)$$

where $\frac{\partial \psi}{\partial n}$, $\frac{\partial \bar{\phi}}{\partial n}$ are directional derivatives along the normal n drawn inward to the surface S and L is Laplacian operator.

Let ψ satisfy

$$L(\psi) = \psi_{xx} + \psi_{yy} + \psi_{zz} = 0 \quad (3.2)$$

the well known Laplace equation in three dimensions. The fundamental solution of this equation is

$$\psi = \frac{1}{4\pi R} \quad (3.3)$$

$$\text{with } R = [(\bar{x} - \xi)^2 + (\bar{y} - \eta)^2 + (\bar{z} - \zeta)^2]^{\frac{1}{2}} \quad (3.4)$$

In cylindrical coordinates we write,

$$\begin{aligned} \bar{y} &= \bar{r} \cos \theta, \quad z = \bar{r} \frac{\sin \theta}{\cos \theta} \\ \eta &= \rho \cos \nu, \quad \zeta = \rho \sin \nu \end{aligned} \quad (3.5)$$

Then (3.4) gives

$$R = [(\bar{x} - \xi)^2 + \bar{r}^2 + \rho^2 - 2\bar{r}\rho \cos(\theta - \nu)]^{\frac{1}{2}} \quad (3.6)$$

Now let us consider the integral identity (3.1) and apply it to the case of axisymmetric flow. We shall treat the volume and surface integrals separately.

VOLUME INTEGRAL

From equation (3.1), the integral over volume V is

$$I_V = \iiint_V [\psi L(\bar{\phi}) - \bar{\phi} L(\psi)] dV \quad (3.7)$$

From equation (3.2) we have $L(\psi) = 0$,

And from equation (2.35)

$$L(\bar{\phi}) = \bar{\phi}_{\bar{x}} - \bar{\phi}_{\bar{x}\bar{x}} = \frac{1}{2} \frac{\partial}{\partial \bar{x}} (\bar{\phi}_{\bar{x}}^2) \equiv \frac{1}{2} \frac{\partial}{\partial \bar{x}} (\bar{u}^2)$$

where $\bar{u} = \bar{\phi}_{\bar{x}}$. Hence equation (3.7) becomes

$$I_V = \frac{1}{2} \iiint_V \psi \frac{\partial}{\partial \xi} (\bar{u}^2) dV \quad (3.8)$$

We integrate (3.8) by parts in ξ -direction. This leads to integral over the bounding surface of the volume V, all of which vanish except that over any shock discontinuity. Thus

$$I_V = \frac{1}{2} \iint_{S_D} \psi \langle \bar{u}^2 \rangle \cos \theta_1 dS - \frac{1}{2} \iiint_V \psi_{\xi} \bar{u}^2 dV \quad (3.9)$$

where $\langle \bar{u}^2 \rangle = \bar{u}_2^2 - \bar{u}_1^2$ is the jump across a shock surface. The upstream unit vector normal to the shock surface is considered as

$$\bar{n} = i \cos \theta_1 + j \cos \theta_2 + k \cos \theta_3$$

and in equation (3.9)

$$\cos \theta_1 \, dS = \text{Sgn}(\cos \theta_1) \rho \, dv \, d\rho = -\rho \, dv \, d\rho$$

Thus we obtain for the volume integral,

$$I_V = -\frac{1}{2} \iint_{S_D} \psi < \bar{u}^2 > \rho \, dv \, d\rho - \frac{1}{2} \iiint_V \bar{\phi} \bar{u}^2 \, dV \quad (3.10)$$

THE SURFACE INTEGRAL

The integral over the body surface S includes (1) the cylindrical surface at infinity, (2) the surface S_p surrounding the singular point $\bar{x}, \bar{y}, \bar{z}$, (3) the surface S_D around any shock discontinuity, and (4) the body surface.

(i) Cylindrical surface at infinity

The integral over the cylindrical surface at infinity can be expressed as

$$\lim_{\rho \rightarrow \infty} \int_0^{2\pi} \int_{-\infty}^{\infty} \left(\bar{\phi} \frac{\partial \psi}{\partial \rho} - \psi \frac{\partial \bar{\phi}}{\partial \rho} \right) \frac{1}{\rho} \, dv \, d\xi$$

This integral, with ψ given by equation (3.3) and with the assumption that $\bar{\phi} \sim \bar{R}^\epsilon$ for $\epsilon > 0$ at infinity, vanishes.

(ii) Integral over S_p surrounding the singular point

Since ψ is singular at the field point $P(\bar{x}, \bar{y}, \bar{z})$, where $R = 0$, it must be excluded from the region of integration. If the surface surrounding the field point is taken as the sphere of radius $R = R_0$, then

$$\psi = \frac{1}{4\pi R_o} \quad \text{and} \quad \frac{\partial \psi}{\partial n} = -\frac{1}{4\pi R_o^2}$$

If ω is the solid angle, the elemental area of the surface is

$$dS = R_o^2 d\omega$$

Thus integration over the surface S_p then gives

$$\begin{aligned} \iint_{S_p} (\bar{\phi} \frac{\partial \psi}{\partial n} - \psi \frac{\partial \bar{\phi}}{\partial n}) dS &= \lim_{R_o \rightarrow 0} \frac{1}{4\pi} \int_0^{4\pi} \left(\frac{\bar{\phi}}{R_o^2} - \frac{1}{R_o} \frac{\partial \bar{\phi}}{R_o} \right) R_o^2 d\omega \\ &= -\bar{\phi}(\bar{x}, \bar{r}) \end{aligned} \quad (3.11)$$

(iii) Integral over shock discontinuity S_D

The quantities ψ , $\frac{\partial \psi}{\partial n}$, $\bar{\phi}$ are continuous across any shock surface, while the normal velocity is discontinuous there. Thus these surfaces are to be excluded from the region of integration in order to apply Green's theorem. The integral over S_D then becomes

$$\iint_{S_D} (\bar{\phi} \frac{\partial \psi}{\partial n} - \psi \frac{\partial \bar{\phi}}{\partial n}) dS = - \iint_{S_D} \left\langle \frac{\partial \bar{\phi}}{\partial n} \right\rangle \psi dS \quad (3.12)$$

where n is the direction of upstream normal to S_D and $\left\langle \frac{\partial \bar{\phi}}{\partial n} \right\rangle$ denotes the jump in $\frac{\partial \bar{\phi}}{\partial n}$ across the shock. Expressing $\left\langle \frac{\partial \bar{\phi}}{\partial n} \right\rangle$ in the form

$$\begin{aligned}
\langle \frac{\partial \bar{\phi}}{\partial n} \rangle &= - \langle \bar{\phi}_{\xi} \rangle \cos \theta_1 - \langle \bar{\phi}_{\rho} \rangle \cos \theta_2 \\
&= -[\langle \bar{u} \rangle \cos \theta_1 + \langle \bar{v} \rangle \cos \theta_2]
\end{aligned}$$

the integral over the shock discontinuity surface S_D , equation (3.12), then becomes

$$\iint_{S_D} \left(\bar{\phi} \frac{\partial \psi}{\partial n} - \psi \frac{\partial \bar{\phi}}{\partial n} \right) dS = \iint_{S_D} [\langle \bar{u} \rangle \cos \theta_1 + \langle \bar{v} \rangle \cos \theta_2] \psi dS \quad (3.13)$$

(iv) Integral over the body surface S_B

$$\iint_{S_B} \left(\bar{\phi} \frac{\partial \psi}{\partial n} - \psi \frac{\partial \bar{\phi}}{\partial n} \right) dS = \lim_{\rho \rightarrow 0} \int_0^{2\pi} \int_0^{\ell} \left[\bar{\phi} \frac{\partial \psi}{\partial \rho} - \psi \frac{\partial \bar{\phi}}{\partial \rho} \right] \rho d\nu d\xi \quad (3.14)$$

From Appendix A, we see that in the limit as $\rho \rightarrow 0$, $\bar{\phi}$ is of the form

$$\bar{\phi} = S'(x) \ln \rho + g_1(x)$$

Also from (3.3) and (3.6) we have

$$\lim_{\rho \rightarrow 0} \frac{\partial \psi}{\partial \rho} = \frac{\bar{r} \cos(\theta - \nu)}{4\pi [(\bar{x} - \xi)^2 + \bar{r}^2]^{3/2}}$$

Hence,

$$\lim_{\rho \rightarrow 0} \bar{\phi}_{\rho} \frac{\partial \psi}{\partial \rho} = 0$$

Thus equation (3.14) reduces to

$$\iint_{S_B} \left(\bar{\phi} \frac{\partial \psi}{\partial n} - \psi \frac{\partial \bar{\phi}}{\partial n} \right) dS = - \lim_{\rho \rightarrow 0} \int_0^{2\pi} \int_0^{\ell} \psi \rho \frac{\partial \bar{\phi}}{\partial \rho} dv d\xi \quad (3.15)$$

Now from the boundary condition (2.36) we see that

$$\lim_{\rho \rightarrow 0} \rho \frac{\partial \bar{\phi}}{\partial \rho} = \frac{(\gamma+1)M_\infty^2}{1 - M_\infty^2} \frac{S'(\xi)}{2\pi} \quad (3.16)$$

and from (3.3) together with (3.6) we have

$$\lim_{\rho \rightarrow 0} \psi = \frac{1}{4\pi [(\bar{x}-\xi)^2 + \bar{r}^2]^{1/2}} \quad (3.17)$$

Substituting (3.15) and (3.16) in (3.14) and simplifying we obtain

$$\iint_{S_B} \left(\bar{\phi} \frac{\partial \psi}{\partial n} - \psi \frac{\partial \bar{\phi}}{\partial n} \right) dS = - \frac{(\gamma+1) M_\infty^2}{(1 - M_\infty^2)} \frac{1}{4\pi} \int_0^{\ell} \frac{S'(\xi)}{\sqrt{(\bar{x}-\xi)^2 + \bar{r}^2}} d\xi \quad (3.18)$$

Finally from equations (3.11), (3.13) and (3.18) we obtain

$$\begin{aligned} \iint_S \left(\bar{\phi} \frac{\partial \psi}{\partial n} - \psi \frac{\partial \bar{\phi}}{\partial n} \right) dS &= - \bar{\phi}(\bar{x}, \bar{r}) + \iint_{S_D} [\langle \vec{u} \rangle \cos \theta_1 + \langle \vec{v} \rangle \cos \theta_2] \psi dS \\ &\quad - \frac{(\gamma+1) M_\infty^2}{(1 - M_\infty^2)} \frac{1}{4\pi} \int_0^{\ell} \frac{S'(\xi)}{\sqrt{(\bar{x}-\xi)^2 + \bar{r}^2}} d\xi \end{aligned} \quad (3.19)$$

INTEGRAL EQUATION FOR VELOCITY POTENTIAL

Substituting equations (3.10) and (3.19) in Green's identity (3.1) we get an integral equation for velocity potential as

$$\begin{aligned} \bar{\phi}(\bar{x}, \bar{r}) = & \frac{-(\gamma+1) M_{\infty}^2}{(1 - M_{\infty}^2)} \frac{1}{4\pi} \int_0^{\ell} \frac{S'(\xi) d\xi}{\sqrt{(\bar{x}-\xi)^2 + \bar{r}^2}} \\ & + \iint_{S_D} [(\langle \bar{u} \rangle - \frac{\bar{u}^2}{2}) \cos \theta_1 + \langle \bar{v} \rangle \cos \theta_2] \psi dS \\ & + \iiint_V \psi \xi \frac{\bar{u}^2}{2} dV \end{aligned} \quad (3.20)$$

Using shock condition (2.38) we see that the integral over the shock discontinuity S_D vanishes. Thus equation (3.20) reduces to

$$\bar{\phi}(\bar{x}, \bar{r}) = - \frac{(\gamma+1) M_{\infty}^2}{1 - M_{\infty}^2} \frac{1}{4\pi} \int_0^{\ell} \frac{S'(\xi)}{\sqrt{(\bar{x}-\xi)^2 + \bar{r}^2}} d\xi + \iiint_V \psi \xi \frac{\bar{u}^2}{2} dV \quad (3.21)$$

which can be written as

$$\bar{\phi}(\bar{x}, \bar{r}) = \bar{\phi}_L + \iiint_V \psi \xi \frac{\bar{u}^2}{2} dV \quad (3.22)$$

where $\bar{\phi}_L = \frac{(\gamma+1) M_{\infty}^2}{1 - M_{\infty}^2} \phi_L$

with $\phi_L = - \frac{1}{4\pi} \int_0^{\ell} \frac{S'(\xi)}{\sqrt{(\bar{x}-\xi)^2 + \bar{r}^2}} d\xi, \quad (3.23)$

ϕ_L being the linear value of the velocity potential.

INTEGRAL EQUATION FOR PERTURBATION VELOCITY

The longitudinal perturbation velocity is given by the \bar{x} -wise derivative of equation (3.21). After isolating the field point by introducing the limits $\xi = \bar{x} \pm \epsilon$, we get,

$$\begin{aligned} \bar{u}(\bar{x}, \bar{r}) &= \frac{\partial}{\partial \bar{x}} \bar{q}_L(\bar{x}, \bar{r}) + \lim_{\epsilon \rightarrow 0} \frac{\partial}{\partial \bar{x}} \iint d\nu d\rho \left[\int_{-\infty}^{\bar{x}-\epsilon} \frac{u^2(\xi, \rho, \nu)}{2} \frac{\partial^2(\psi)}{\partial \xi^2} d\xi + \int_{\bar{x}+\epsilon}^{\infty} \frac{u^2(\xi, \rho, \nu)}{2} \frac{\partial^2(\psi)}{\partial \xi^2} d\xi \right] \\ &= \bar{u}_L(\bar{x}, \bar{r}) + \lim_{\epsilon \rightarrow 0} \frac{1}{2\pi} \iint \frac{\bar{u}^2(x; \rho, \nu)}{2} \frac{\epsilon d\nu d\rho}{[\epsilon^2 + \bar{r}^2 + \rho^2 - 2\bar{r}\rho \cos(\theta - \nu)]^{3/2}} \\ &\quad - \iiint_V \frac{1}{2} \bar{u}^2(\xi, \rho, \nu) \frac{\partial^2(\psi)}{\partial \xi^2} dV \quad (3.24) \end{aligned}$$

In the limit as $\epsilon \rightarrow 0$, the influence function in the integrand of the above double integral is effectively a two dimensional pulse function at the point $\rho = \bar{r}$, $\theta = \nu$ and of strength 2π [see Heaslet (1956)] The expression for u then becomes,

$$\bar{u}(\bar{x}, \bar{r}) = \bar{u}_L(\bar{x}, \bar{r}) + \frac{\bar{u}^2}{2}(\bar{x}, \bar{r}) - \iiint_V \frac{\bar{u}^2}{2}(\xi, \rho, \nu) \frac{\partial^2(\psi)}{\partial \xi^2} dV \quad (3.25)$$

consider the volume integral in equation (3.24)

$$\begin{aligned} \iiint_V \frac{\bar{u}^2}{2} \frac{\partial^2(\psi)}{\partial \xi^2} dV &= \frac{1}{4\pi} \int_{-\infty}^{\infty} \int_0^{\infty} \int_0^{2\pi} d\nu d\rho d\xi \frac{\bar{u}^2}{2}(\xi, \rho, \nu) \\ &\quad \frac{\partial^2}{\partial \xi^2} \left[\frac{1}{\sqrt{(\bar{x}-\xi)^2 + \bar{r}^2 + \rho^2 - 2\bar{r}\rho \cos(\theta - \nu)}} \right] . \end{aligned}$$

For axisymmetric flow and small $\bar{r}(\bar{r} \rightarrow 0)$, we obtain

$$\iiint_V \frac{\bar{u}^2}{2} \frac{\partial^2(\psi)}{\partial \xi^2} dV = \frac{1}{2} \int_{-\infty}^{\infty} \int_0^{\infty} \frac{\bar{u}^2}{2}(\xi, \rho) \frac{\partial^2}{\partial \xi^2} \left(\frac{\rho}{\sqrt{(\bar{x}-\xi)^2 + \rho^2}} \right) d\rho d\xi \quad (3.26)$$

Substituting equation (3.26) in (3.24), we obtain for axisymmetric flow

$$\begin{aligned} \bar{u}(\bar{x}, \bar{r}) = & \bar{u}_L(\bar{x}, \bar{r}) + \frac{\bar{u}^2}{2}(\bar{x}, \bar{r}) \\ & - \frac{1}{2} \int_{-\infty}^{\infty} \int_0^{\infty} \frac{\bar{u}^2}{2}(\xi, \rho) \frac{\partial^2}{\partial \xi^2} \left(\frac{\rho}{\sqrt{(\bar{x}-\xi)^2 + \rho^2}} \right) d\rho d\xi \end{aligned} \quad (3.27)$$

This is then the final form of integral equation for transonic flow past slender bodies of revolution.

3.3 SIMPLIFICATION OF INTEGRAL EQUATION

In solving the integral equation (3.24) the difficulty arises due to the kernel of the double integral. Hence we introduce further simplification. We assume a functional relationship

$$\bar{u}(\bar{x}, \bar{r}) = \bar{u}(\bar{x}, 0) e^{\bar{r}/b} \quad (3.28)$$

between the velocity on the body surface and the velocity directly above the surface of the body in a similar manner as for the two dimensional case [see Norstrud (1973)]. This relationship satisfies the condition of zero disturbance at infinity. In order that (3.28) also satisfy the boundary condition at the body surface, we determine

b as follows. We differentiate equation (3.28) with respect to \bar{r} and set $\bar{r} = 0$, hence

$$\left(\frac{\partial \bar{u}}{\partial \bar{r}} \right)_{\bar{r}=0} = - \frac{\bar{u}(\bar{x}, 0)}{b}$$

$$\text{so that } b = \frac{-\bar{u}(\bar{x}, 0)}{\left(\frac{\partial \bar{u}}{\partial \bar{r}} \right)_{\bar{r}=0}}$$

$$= - \frac{\bar{u}(\bar{x}, 0)}{\left(\bar{\phi}_{\bar{x}\bar{r}} \right)_{\bar{r}=0}}.$$

Now $\left(\bar{\phi}_{\bar{x}\bar{r}} \right)_{\bar{r}=0}$ can be determined by using the boundary condition (2.36) which gives on the body surface

$$\lim_{\bar{r} \rightarrow 0} \bar{\phi}_{\bar{x}\bar{r}} = \frac{(\gamma+1)M_\infty^2}{1-M_\infty^2} R''(x)$$

Thus

$$b = - \frac{(\gamma+1)M_\infty^2}{(1-M_\infty^2)} \frac{\bar{u}(\bar{x}, 0)}{R''(x)} \quad (3.29)$$

Substituting relation (3.28) into (3.27), we get

$$\begin{aligned} \bar{u}(\bar{x}, 0) e^{\bar{r}/b} &= \bar{u}_L(\bar{x}, \bar{r}) + \frac{1}{2} \bar{u}^2(\bar{x}, 0) e^{2\bar{r}/b} \\ &\quad - \frac{1}{2} \int_{-\infty}^{\infty} \frac{\bar{u}^2(\xi, 0)}{2} \frac{\partial^2}{\partial \xi^2} \int_0^\infty \frac{\rho e^{-2\rho/b}}{\sqrt{(\bar{x}-\xi)^2 + \rho^2}} d\rho d\xi \end{aligned}$$

which in the limit as $\bar{r} \rightarrow 0$, gives

$$\bar{u}(\bar{x}, 0) = \bar{u}_L(\bar{x}, 0) + \frac{1}{2} \bar{u}^2(\bar{x}, 0) - \frac{1}{2} \int_{-\infty}^{\infty} \frac{\bar{u}^2(\xi, 0)}{2b} E(|\bar{x} - \xi|; b) d\xi \quad (3.30)$$

where $E(|\bar{x} - \xi|; b)$ is the influence coefficient defined as
(see Appendix B)

$$\begin{aligned} E(|\bar{x} - \xi|; b) &= b \frac{\partial^2}{\partial \xi^2} \left(\int_0^{\infty} \frac{e^{-2\rho/b}}{\sqrt{(\bar{x} - \xi)^2 + \rho^2}} d\rho \right) \\ &= 2\pi \left[\{H_1'(Z) - N_1'(Z)\} + \frac{Z}{2} \{H_1''(Z) - N_1''(Z)\} \right] \end{aligned}$$

with $Z = \frac{2|\bar{x} - \xi|}{b}$.

3.4 SYSTEM OF ALGEBRAIC EQUATIONS

The integral appearing in equation (3.30) is solved by quadrature, by approximating the range of integration with a finite number N discrete intervals and letting the unknown function $\bar{u}(\bar{x}, 0)$ be represented by a mean value within each element. For points ahead of the leading edge ($\bar{x} < 0$) or for points aft of the trailing edge ($\bar{x} > l$) the expression for $\bar{u}(\bar{x}, 0)$ as described by (3.30) is going to be identically zero. Thus it is presumed in effect that the influence from points upstream and downstream of the body on the value of $\bar{u}(\bar{x}, 0)$ can be neglected. Thus equation (3.30) can be replaced by the following system of nonlinear algebraic equations.

$$\bar{u}_i = \bar{u}_{L_i} + \frac{1}{2} \bar{u}_i^2 - \frac{1}{4} \sum_{j=1}^N \epsilon_{ij} \bar{u}_j^2 \quad (3.31)$$

$$i = 1, 2, \dots, N.$$

where the influence coefficients ϵ_{ij} are integral functions of E and are defined as

$$\begin{aligned} \epsilon_{ij} &= \frac{1}{b_j} \int_{\bar{x} - \frac{\Delta \bar{x}}{2}}^{\bar{x} + \frac{\Delta \bar{x}}{2}} E \, d\bar{x} \\ &= \frac{\Delta \bar{x}}{b_j} E(|\bar{x}_i - \bar{x}_j|; b_j) \end{aligned}$$

Rewriting equation (3.31) we obtain

$$\bar{u}_i - \frac{1}{2} \bar{u}_i^2 - \bar{u}_{L_i} + \frac{1}{4} \sum_{j=1}^N \epsilon_{ij} \bar{u}_j^2 = 0 \quad (3.32)$$

$$i = 1, 2, \dots, N.$$

3.5 APPLICATION OF THE METHOD OF PARAMETRIC DIFFERENTIATION

The method of parametric differentiation is applied to the system of equations (3.32). We introduce a parameter μ , say artificial viscosity, such that

$$F_i(\bar{u}_i(\mu, \mu)) = \bar{u}_i - \bar{u}_{L_i} - \mu \left[\frac{1}{2} \bar{u}_i^2 - \frac{1}{4} \sum_{j=1}^N \epsilon_{ij} \bar{u}_j^2 \right] = 0 \quad (3.33)$$

$$i = 1, 2, \dots, N.$$

Differentiation of (3.33) is performed with respect to μ , which yields a system of first order nonlinear ordinary differential equations.

$$\frac{d\bar{u}_i}{d\mu} = \frac{1}{(1 - \mu\bar{u}_i)} \left[\frac{1}{2} \bar{u}_i^2 - \frac{1}{2} \sum_{j=1}^N \epsilon_{ij} (\bar{u}_j^2 + 2\mu\bar{u}_j \frac{d\bar{u}_j}{d\mu}) \right] \quad (3.34)$$

$$i = 1, 2, \dots, N.$$

Here we have considered \bar{u}_{L_i} independent of μ , so that $\bar{u}_i = \bar{u}_{L_i}$ at $\mu = 0$ and $\bar{u}_i = \bar{u}_i(\mu)$ is unknown.

The unknown vector u_i can be found out from differential equations (3.34) as the solution to the defined Cauchy's problem at $\mu = 1$, with the initial vector solution

$$\bar{u}_i = \bar{u}_{L_i} \quad \text{at } \mu = 0 \quad (3.35)$$

The condition for a unique solution of the system (3.34) in the range $0 \leq \mu \leq 1$ is the non-vanishing of the functional determinant or Jacobian of $F_i[\bar{u}_i(\mu), \mu]$ with respect to \bar{u}_i for fixed μ . The Jacobian matrix of the system is given by

$$J(\bar{u}_1, \bar{u}_2, \dots, \bar{u}_N) = \frac{\partial(F_1, \dots, F_N)}{\partial(\bar{u}_1, \dots, \bar{u}_N)} \quad (3.36)$$

The Jacobian matrix (3.36) is positive definite under the condition that the elements on the principle diagonal are positive i.e.,

$$(1 - \mu\bar{u}_i) > 0$$

$$\bar{u}_i < \mu^{-1}, \quad i = 1, 2, \dots, N.$$

For a certain value of $\max [\bar{u}_i^{-1}]$, however, the Jacobian matrix becomes singular and the solution curve of the Cauchy problem can split into two or more solutions. Such a point $\mu = \mu^*$ in the interval $0 \leq \mu \leq 1$ for which

$$\det J(\bar{u}_1, \bar{u}_2, \dots, \bar{u}_N) = 0$$

can be treated as a bifurcation point and the associated solution $\bar{u}_i^* = \bar{u}_i(\mu^*)$ will be designated as the bifurcation solution.

After obtaining numerically a unique and real solution $\bar{u}_i = \bar{u}_i(\mu)$ to the set of differential equations (3.34), using Hamming's predictor-corrector method, at $\mu^* \leq 1$, which represents within some error bounds, the best possible approximation to the condition of minimum bifurcation, the next step will involve crossing of the singular Jacobian matrix. Therefore a continuous dependence of the solution on the initial data is no longer possible.

In order to solve the system (3.33) at $\mu = 1$, method of steepest descent is used. The values at the minimum bifurcation point is assumed as the initial values for the steepest descent method.

For subcritical and continuous supercritical flows the velocity distribution obtained at the point of minimum bifurcation is assumed as the initial velocity distribution. But for discontinuous supercritical flow the velocity distribution at the point of minimum bifurcation is assumed with a shock discontinuity. This is so because we cannot obtain a discontinuous solution by assuming the continuous solution as the initial condition for steepest descent method.

CHAPTER 4

LOCAL LINEARIZATION METHOD

4.1 INTRODUCTION

In this chapter method of local linearization due to Spreiter and Alksne (1959) has been discussed. In section 4.2 details of the method as applied to axisymmetric flows has been given. Section 4.3 deals with modification of local linearization technique as suggested by Fink (1971). In section 4.4 an empirical approximation for shock wave location and its strength is given. Section 4.5 gives method of solution of the equations obtained by application of the local linearization technique.

4.2 APPLICATION OF LOCAL LINEARIZATION TECHNIQUE TO AXISYMMETRIC FLOWS

The nonlinear differential equation for axisymmetric flow is

$$(1-M_\infty^2)\phi_{xx} + \frac{1}{r}\phi_r + \phi_{rr} = M_\infty^2(\gamma+1)\phi_x\phi_{xx} = k\phi_x\phi_{xx} \quad (4.2.1)$$

The local linearization technique is applied to equation (4.2.1) for locally subsonic, locally supersonic and near sonic flows. The three cases are discussed separately in the following .

(i) Locally subsonic case

It is convenient to introduce λ_E for the coefficient of ϕ_{xx} in equation (4.2.1), which is then rewritten in the form

$$\lambda_E \phi_{xx} + \frac{1}{r} \phi_{xr} + \phi_{rr} = 0 \quad (4.2.2)$$

where $\lambda_E = 1 - M_\infty^2 - ku$. It is now assumed that λ_E is neither zero nor infinite and that it varies sufficiently slowly that its derivatives can be disregarded so that it can be considered, temporarily, as a constant. The problem is now similar to that in linearized theory of subsonic flow past slender bodies of revolution. The solution of equation (4.2.2) subject to appropriate B.C. on the body surface and at infinity is thus given by [see e.g. Ward, G.N. (1955)]

$$\phi_E = - \frac{1}{4\pi} \int_0^l \frac{S'(\xi) d\xi}{\sqrt{(x-\xi)^2 + \lambda_E^2 r^2}} \quad (4.2.3)$$

The expression for velocity u_E follows by differentiation of (4.2.3). It can be approximated for points on the surface of smooth slender body by

$$\begin{aligned} u_E &= \frac{S''(x)}{4\pi} \ln \frac{\lambda_E S}{4\pi x(l-x)} + \frac{1}{4\pi} \int_0^l \frac{S''(x) - S''(\xi)}{|x - \xi|} d\xi \\ &= \frac{S''(x)}{4\pi} \ln \lambda_E + u_i \end{aligned} \quad (4.2.4)$$

where subscript i refers to the values for incompressible flow $M_\infty = 0$. Differentiation of (4.2.4) yields,

$$\frac{du_E}{dx} = \frac{S'''(x)}{4\pi} \ln \lambda_E + \frac{du_i}{dx} \quad (4.2.5)$$

Now, $1 - M_\infty^2 - ku$ is restored in place of λ_E so that, in effect, the local value for λ_E is used at each point and the subscript on u is dropped. Then equation (4.2.5) becomes

$$\begin{aligned} \frac{du}{dx} &= \frac{S''(x)}{4\pi} \ln(1 - M_\infty^2 - ku) + \frac{du_i}{dx} \\ &\equiv F(x, u) \end{aligned} \quad (4.2.6)$$

Equation (4.2.6) is a nonlinear ordinary differential equation of first order for u on the body surface which is solved using the condition

$$u = u_i \quad \text{at } S''(x) = 0 \quad (4.2.7)$$

(ii) Locally supersonic case

In this case we introduce λ_H for the coefficient of ϕ_{xx} so that equation (4.2.1) reduces to

$$\lambda_H \phi_{xx} - \frac{1}{r} \phi_r - \phi_{rr} = 0 \quad (4.2.8)$$

where $\lambda_H = M_\infty^2 - 1 + ku$. It is again assumed that λ_H is neither zero nor infinite and that it varies sufficiently slowly that its derivatives can be disregarded. The problem is then equivalent to that encountered in linearized supersonic slender body theory. The solution for ϕ for points on the surface of a smooth slender pointed body of revolution is given by [see e.g. Ward, G.N.(1955)]

$$\phi_H = - \frac{1}{2\pi} \int_0^{x-\sqrt{\lambda_H}r} \frac{S'(\xi) d\xi}{\sqrt{(x-\xi)^2 - \lambda_H r^2}} \quad (4.2.9)$$

The corresponding expression for u_H can be approximated for points on the surface of a smooth slender body by

$$\begin{aligned} u_H &= \frac{S''(x)}{4\pi} \ln \frac{\lambda_H S}{4\pi x^2} + \frac{1}{2\pi} \int_0^x \frac{S''(x) - S''(\xi)}{x - \xi} d\xi \\ &= \frac{S''(x)}{4\pi} \ln \lambda_H + f_H(x) \end{aligned} \quad (4.2.10)$$

$$\text{where } f_H(x) = \frac{S''(x)}{4\pi} \ln \frac{S(x)}{4\pi x^2} + \frac{1}{2\pi} \int_0^x \frac{S''(x) - S''(\xi)}{x - \xi} d\xi \quad (4.2.11)$$

$f_H(x)$ can be interpreted as the linear value of u for $M_\infty = \sqrt{2}$.

Differentiation of (4.2.10) gives

$$\frac{du_H}{dx} = \frac{S'''(x)}{4\pi} \ln \lambda_H + \frac{df_H(x)}{dx} \quad (4.2.12)$$

If, now $M_\infty^2 - 1 + ku$, is restored in place of λ_H so that, in effect, the local value for λ_H is used at each point and the subscript H on u is dropped, equation (4.2.12) becomes

$$\frac{du}{dx} = \frac{S'''(x)}{4\pi} \ln (M_\infty^2 - 1 + ku) + \frac{df_H(x)}{dx} \quad (4.2.13)$$

$$\equiv F(x, u)$$

Equation (4.2.13) is a nonlinear first order ordinary differential equation for u on the body surface which may be solved using

$$u = f_H \quad \text{at} \quad S''(x) = 0 \quad (4.2.14)$$

as the starting condition.

(iii) Locally near sonic case

The analyses of subsonic and supersonic cases as described above have started by introduction of a symbol λ for the coefficient of ϕ_{xx} and the assumption that λ is neither zero nor infinite and that it varies sufficiently slowly that it can be regarded as a constant in the early stages of the analysis. Since the results so obtained terminate if $\lambda = 0$, i.e., if a point is approached at which the velocity is sonic, it is evident that additional considerations are necessary to study the flows with free-stream Mach number near one in which the acceleration from subsonic to supersonic velocities is an essential feature.

In this case λ_p is chosen for the coefficient of ϕ_x rather than ϕ_{xx} . Thus equation (4.2.1) becomes

$$\frac{1}{r} \phi_r + \phi_{rr} - \lambda_p \phi_{xx} = (M_\infty^2 - 1) \phi_{xx} = f_p \quad (4.2.15)$$

where $\lambda_p = M_\infty^2 (\gamma + 1) \phi_{xx} = k \frac{\partial u}{\partial x}$. It is assumed, once again that,

λ_p is nonsingular and that it varies sufficiently slowly that it can be considered constant in the initial stages of the analysis.

Now considering λ_p positive and constant, with the use of boundary conditions [equation (2.23)] and the Green's theorem associated with the L.H.S. of equation (4.2.15) yields

$$\phi_p = - \frac{1}{4\pi} \int_0^x \frac{S'(\xi)}{x - \xi} d\xi + \frac{-\lambda_p r^2}{4(x-\xi)} d\xi - \frac{1}{\lambda_p} \int_0^{2\pi} dv \int_0^\infty \rho d\rho \int_{-\infty}^x \sigma_\rho f_p d\xi \quad (4.2.16)$$

$$\text{where } \sigma_p = \frac{\lambda_p}{4\pi(x-\xi)} e^{-\frac{\lambda_p[\gamma^2 + \rho^2 - 2\gamma\rho \cos(\theta-\nu)]}{4(x-\xi)}} \quad (4.2.17)$$

Now, $u_p = \frac{\partial \phi_p}{\partial x}$ can be approximated for points on the surface of a smooth slender body by

$$u_p = \frac{S''(x)}{4\pi} \ln \frac{\lambda_p S e^C}{4\pi x} - \frac{1}{4\pi} \int_0^x \frac{S''(x) - S''(\xi)}{x - \xi} d\xi - \frac{1}{\lambda_p} \frac{\partial}{\partial x} \int_0^2 \rho v \int_0^\infty \rho d\rho \int_{-\infty}^x f_p \sigma_p d\xi \quad (4.2.18)$$

where $C = \text{Euler's constant} \approx 0.577215$.

If the free stream Mach number is unity f_p vanishes and u_p can be calculated directly. If the free-stream Mach number is not unity, the equation (4.2.18) is an integral equation. However for Mach numbers near unity, it is only necessary to approximate $\phi_{\xi\xi}$ locally by substituting λ_p/k for $\phi_{\xi\xi}$ or $\partial u/\partial \xi$ in the tripple integral. Doing so and evaluating the integral in (4.2.18), we get

$$u_p = \frac{1 - M_\infty^2}{(\gamma+1)M_\infty^2} + \frac{S''(x)}{4\pi} \ln \frac{\lambda_p S e^C}{4\pi x} + \frac{1}{4\pi} \int_0^x \frac{S''(x) - S''(\xi)}{x - \xi} d\xi \quad (4.2.19)$$

If, once again, $k \frac{\partial u}{\partial x}$ is restored in place of λ_p , the subscript P is dropped, and use is made of the following relation between $\frac{\partial u}{\partial x}$

and $\frac{du}{dx}$ along the surface of the body

$$\begin{aligned} \frac{d(u)_R}{dx} &= \left[\frac{\partial(u)}{\partial x} \right]_R + \left[\frac{\partial(u)}{\partial r} \right]_R \frac{dR}{dx} \\ &= \left[\frac{\partial u}{\partial x} \right]_R + \frac{S' S''}{4\pi S} \end{aligned} \quad (4.2.20)$$

a nonlinear ordinary differential equation is obtained for u on the body surface. It is

$$\begin{aligned} u &= \frac{1 - M_\infty^2}{(\gamma + 1) M_\infty^2} + \frac{S''(x)}{4\pi} \ln \left\{ \left[\frac{du}{dx} - \frac{S' S''}{4\pi S} \right] \left[\frac{(\gamma + 1) M_\infty^2 S e^C}{4\pi x} \right] \right\} \\ &\quad + \frac{1}{4\pi} \int_0^x \frac{S''(x) - S''(\xi)}{x - \xi} d\xi \end{aligned}$$

Rearranging we obtain

$$\frac{du}{dx} = \frac{S' S''}{4\pi S} + \frac{2}{(\gamma + 1) M_\infty^2 S e^C} \exp \left\{ \frac{4\pi}{S} [u + G - f_H/2] \right\} \quad (4.2.21)$$

where $G(M_\infty, \gamma) = \frac{M_\infty^2 - 1}{(\gamma + 1) M_\infty^2}$ and f_H is as defined in equation (4.2.11).

Again we see that equation (4.2.21) is of the form

$$\frac{du}{dx} = F(x, u) \quad (4.2.22)$$

To obtain a finite velocity gradient at the point where

$S'' = 0$, it is necessary to assume that

$$(u)_{S''=0} = \frac{1}{2} (f_H)_{S''=0} - G \quad (4.2.23)$$

As with the cases for fully subsonic and supersonic flows, the value of u at this axial station then serves as the initial condition for the solution of equations (4.2.6) and (4.2.13). At this station, equation (4.2.21) becomes

$$\left(\frac{du}{dx}\right)_{S''=0} - \frac{S'''}{4\pi} \ln \left(\frac{du}{dx}\right)_{S''=0} = \frac{1}{2} \left(\frac{df_H}{dx}\right)_{S''=0} + \frac{S'''}{4\pi} \ln \left[\frac{(\gamma+1)M_{\infty}^2}{2} \right] \quad (4.2.24)$$

from which the velocity gradient at the starting point is computed.

The term G arises from a complicated volume integral in equation (4.2.18). It is evaluated therein by use of approximations valid only for Mach numbers very close to one. Agreement between calculated results and experimental data is best at Mach number one, where G is zero and becomes poor as G increases in magnitude.

Equations (4.2.6), (4.2.13) and (4.2.21) are first order ordinary differential equations which can be solved using the initial conditions as specified in the respective sections. The coefficient of pressure C_p on the body surface can be calculated by using equation (2.24a),

$$C_p = -2u - \left(\frac{dR}{dx}\right)^2 \quad (4.2.25)$$

4.3 FINK'S MODIFICATION

Fink suggested that if a revised solution is to be meaningful at high transonic speeds G in equation (4.2.21) should

approach $-\frac{1}{2}(f_H)''_{S=0}$ with increasing M_∞ so that the velocity given by equation (4.2.23) would approach that of linearized supersonic theory. Similarly, G should approach $-(u_i)''_{S=0} + \frac{1}{2}(f_H)''_{S=0}$ with decreasing transonic Mach number. The behaviour of G with M_∞ is shown in Fig. 14. It is seen that very near a Mach number of one, G depends on M_∞ and is independent of body shape. Away from one, G depends on body shape, is inversely proportional to fineness ratio squared and is independent of M_∞ and γ . The simplest function which has this behaviour is for $M_\infty \leq 1$,

$$G = \frac{1}{2}(f_H - 2u_i)''_{S=0} \{ 1 - \exp[-\chi_\infty / (f_H/2\tau^2) - u_i/\tau^2] \}''_{S=0} \quad \dots (4.3.1)$$

for $M_\infty \geq 1$,

$$G = -\frac{1}{2}(f_H)''_{S=0} \{ 1 - \exp[\chi_\infty / (f_H/2\tau^2)] \}''_{S=0} \quad \dots (4.3.2)$$

where $\chi_\infty = \frac{(M_\infty^2 - 1)}{(\gamma + 1)M_\infty^2 \tau^2}$ is the transonic similarity parameter.

With G defined by equation (4.3.1) or (4.3.2) the different solutions are patched to obtain the final pressure distribution. This has been discussed in section 4.5.

4.4 SHOCK WAVE APPROXIMATION

At a Mach number one the shock wave is assumed to be at the after body location where $S'' = 0$. From inspection of measured

variations of shock wave location with low transonic Mach number it was assumed that shock wave location varied linearly with the transonic similarity parameter X_∞ . It is then interpolated linearly from the minimum pressure location at the lower critical similarity parameter to the point $S'' = 0$ on the after body at $M_\infty = 1$.

The shock wave strength is also empirically determined. The shock wave is arbitrarily assumed to produce a downstream axial component of Mach number equal to 0.999. Thus the axial component of perturbation velocity downstream of the shock wave is empirically taken as

$$u_2 = \frac{(0.999 - M_\infty^2)}{(\gamma + 1) M_\infty^2} \quad (4.4.1)$$

4.5 METHOD OF SOLUTION

For purely subsonic flows the differential equation (4.2.6) is integrated with the starting condition given by (4.2.7), upto some point near the nose and then returned to the starting point X_S and integrated towards the tail. The calculations cannot be carried right to the nose or tail as there is a logarithmic singularity at these locations. For purely supersonic flows the differential equation (4.2.13) ^{is} integrated with the starting condition given by (4.2.14). The integration is first done towards the nose and then returned to the starting point X_S and continued towards the tail.

For the cases of purely subsonic and supersonic flows the condition at the starting point is sufficient to determine a unique solution. But additional considerations are necessary for accelerating transonic flows. This is so because the differential equation (4.2.21) is singular at the point, X_S where $S''(X)$ vanishes. Consequently, there exist an infinite number of integral curves which pass through that point. Of all these curves, however, only one is analytic (all derivatives finite) and selection of it suffices to determine a unique solution. This assures that the solution for u/U_∞ can be expanded in a Taylor series in the neighbourhood of the point where $S''(X)$ vanishes. The gradient at the neighbouring points of X_S is calculated using equation (4.2.21). This is compared with the gradient calculated by equation (4.2.6). The equation which gives smaller velocity gradient is considered and the solution is continued to some point near the nose. Now, the solution returns to the point X_S , where the velocity gradient from equation (4.2.21) is compared with that from equation (4.2.13). The equation which gives smaller velocity gradient is considered and the solution is continued towards the tail.

Thus the solution starts with transonic accelerating flows given by equation (4.2.21), which is patched to subsonic local linearization solution given by equation (4.2.6) towards the nose and to supersonic local linearization solution given by

equation (4.2.37) towards the tail. The deceleration from supersonic to subsonic local linearization may occur either through a shock wave as explained in section (4.4) or smooth deceleration through sonic velocity whichever is calculated to occur first.

In each of the preceding steps all differential equations are integrated using Hamming's predictor-corrector method, with the initial values calculated by Runge-Kutta method.

CHAPTER 5

COMPUTATIONAL DETAILS, RESULTS AND DISCUSSION

5.1 INTRODUCTION

The computational details for the method used in solving the system of equations (see Chapters 3 and 4) are given and discussion of results obtained is presented. Results are computed for parabolic arc body of revolution of different fineness ratios at different free stream Mach numbers, by integral equation approach and the method of local linearization. The results are compared with the experimental data given by Taylor (1958) and the more accurate numerical results calculated by Bailey (1971) using a relaxation procedure.

5.2 INTEGRAL EQUATION APPROACH

5.2.1 COMPUTATIONAL DETAILS

The flow chart is shown in Fig. 4. Listing of the computer program is given in Appendix C. Definition of the variables used in the program is given in the listing. The equation for the parabolic arc body of revolution is denoted by $YP(A)$. The subroutine LINEAR calculates the linear velocity distribution UBR using equation (4.2.4) with λ_E replaced by $1 - M_\infty^2$. For applying the Hamming's

predictor-corrector method the initial values are calculated by Runge-Kutta method. The initial condition for Runge-Kutta method is taken at $\mu = 0$ with $U = UBR$. The subroutine DERIV calculates the velocity derivative F . In DERIV subroutine INCOEF is called which calculates the influence coefficient E , given by equation (3.27a). In Hamming's predictor-corrector method, first the solution vector is predicted which is denoted by USP. This predicted solution is modified and Hamming's corrector is applied. A convergence test is applied at each step so that the values are within the prescribed error bound. After calculating the final velocity distribution USN, at different AMEW ($= \mu$), a check has been applied for the Jacobian matrix. If USN is less than $(AMEW)^{-1}$ the process of integration is continued, otherwise, the method of steepest descent is applied to solve the system. For continuous flows the initial values for the steepest descent method are those at which the Jacobian matrix becomes singular. For discontinuous flows the procedure shown in Fig. 6 is followed. The linear velocity distribution and the velocity distribution obtained at the bifurcation point is shown in the figure. In order to assume a discontinuous solution at the bifurcation point guidance from existing results is taken. The assumed velocity distribution, which is now discontinuous is also shown in Fig. 6. These values are denoted by URR in the program. The steepest descent method is now applied through the subroutine STEEP. In STEEP subroutines

FUNVAL and GRAD are called which calculate the functional value and gradient of functional value of equation (3.33) respectively. From the bifurcation point the iteration by steepest descent method is carried upto $AMEW = 1$ to get the final velocity distribution. The pressure distribution CPP is calculated at different points along the length of the body corresponding to the final velocity distribution.

5 2.2 RESULTS AND DISCUSSION

Results are obtained for a parabolic arc body of fineness ratio 10 at Mach numbers 0.7, 0.8 which represent subcritical cases, and at 0.9 which represents supercritical continuous case. Results are also computed for a body of fineness ratio 10 at Mach numbers 0.95, 0.975 and 0.990 which represent, supercritical discontinuous cases. Results at $M_\infty = 0.8$ and 0.95 for a body of fineness ratio 10, 12, 14 are also computed.

The behaviour of influence coefficient E is shown in Fig. 5. Fig. 7 shows the comparison of results obtained for a body of fineness ratio 10 at $M_\infty = 0.9$ with the experimental results of Taylor and numerical results of Bailey. It is observed that the results obtained by integral equation approach are in good agreement with the experimental data near the fore and aft of the body. But the agreement is not so good in the central region. Fig. 8

and Fig. 9 show the comparison of results obtained for a body of fineness ratio 10 at Mach numbers. 0.975 and 0.99, with the experimental and numerical results. It can be seen from figures 8 and 9 that the results agree well with the experimental and numerical results for the fore and aft part of the body. The location of the shock is also predicted closely to that given by numerical results. The results, however, diverge just ahead of the shock.

This divergence may be attributed to the assumed functional relationship [see equation (3.28)] which represents the transverse variation of velocity in terms of the velocity on the body surface. This approximation although quite adequate for subcritical flows, may not be accurate enough to give satisfactory results for supercritical flows when shocks are present [see Nixon (1975)]. The accuracy of the numerical results may be due to the fact that they make use of boundary conditions to approximate inviscid flow in open-jet and porous-wall wind-tunnel sections. These take care of wall induced interference effects. In the integral equation approach we have not considered such effects.

Figure 10 shows the Mach number effect on a body of fixed fineness ratio 10 at Mach numbers 0.7, 0.8 and 0.9, while Fig. 11 gives the results at Mach numbers 0.95, 0.975 and 0.99. It is seen that with the increase in Mach number the pressure coefficient

decreases over the central portion of the body and the location of the shock wave moves towards the tail as the Mach number increases. Fig. 12 shows the results obtained at $M_\infty = 0.8$ for fineness ratios 10, 12 and 14 showing thickness effect. We observe that as the fineness ratio increases, the pressure coefficient decreases over the central portion of the body. From Fig. 13 it can be seen that as fineness ratio decreases the shock location moves towards the tail.

5.3 LOCAL LINEARIZATION METHOD

5.3.1. COMPUTATIONAL DETAILS

The flow chart and listing of the program is given in Fig.14a and Appendix D respectively. The various variables used are described in the listing. To start with we have to solve equation (4.2.24) to calculate the velocity gradient at the point X_s , where $S'(x)$ vanishes. This is achieved by method of successive approximations [see Carnahan (1969)] . Now the velocity at the neighbouring points of X_s is predicted using Taylor's expansion. The solution is continued from these neighbouring points to some point near the nose and to some point near the tail by integrating differential equations, (4.2.6), (4.2.13) and (4.2.21). For this Hamming's predictor-corrector method is applied through the subroutine HAMING. In HAMING subroutine REMY is called, which calculates necessary initial values for the predictor-corrector method by Runge-Kutta method. In REMY subroutine VENU is called which calculates the derivative F. In HAMING first the solution vector is

predicted which is denoted by YP in the program. YMI represents the modified value of YP. Hamming's corrector is applied to this modified value YMI. A convergence test is applied at each step to keep the errors within a prescribed limit.

As explained in section 5 of Chapter 4 we need to match the different solutions for which we compare the gradients. The subroutine DELTA calculates the velocity gradients and these gradients are compared to decide the solution to be used. The variable NCAS indicates the equation being integrated at each step. After obtaining the velocity distribution, the pressure distribution is calculated.

5.3.2 RESULTS AND DISCUSSION

Results are once again obtained for a body of fineness ratio 10 at Mach numbers 0.7 and 0.8, which are subcritical cases, for 0.9, which is a supercritical continuous case and for 0.95, 0.975, 0.99, 1.01 and 1.025 which are supercritical discontinuous cases. The results are also computed for purely supersonic Mach numbers 1.05, 1.075, 1.10 and 1.20.

Fig. 14 gives the behaviour of G with Mach number. The results of local linearization method for fineness ratio 10 at Mach numbers 0.7, 0.8, 0.9 and 0.95, 0.975, 0.990 are compared in Fig. 15 and Fig. 16 with the experimental data and the results obtained by integral equation approach.

We see that the results of local linearization is in good agreement with the experimental data. The results of integral equation approach for subcritical Mach numbers seem to be in good agreement with experimental data, but the agreement becomes poor as the Mach number increases. The shock location predicted by the integral equation approach for $M_\infty = 0.95$ and $M_\infty = .975$ is upstream of that predicted by the local linearization technique. But for $M_\infty = 0.990$ the shock location obtained by the integral equation approach is slightly downstream of that predicted by the local linearization method and the experimental results. The shock location and the shock strength in the local linearization method is obtained empirically while in the case of integral equation approach the strength and the location of the shock is obtained as a solution of the problem.

Pressure distribution for supersonic Mach numbers 1.01, 1.025, 1.075, 1.10 and 1.20 are also calculated and are presented in Figs. 17 and 18.

We observe that the method of local linearization is more versatile in the sense that it can handle the whole range of Mach numbers from subsonic to low supersonic and gives reasonably accurate results.

5.4 CONCLUSIONS

To conclude we see that the integral equation approach is well suited for solving the problem of axisymmetric transonic flow past slender bodies. We have been successful in formulating the problem in the same manner as done for two dimensional case. The accuracy of the results obtained by the integral equation approach is of the same order as that obtained for the two-dimensional case. The location of the shock wave as predicted by the integral equation approach is close to the one predicted by the experimental data and the more exact numerical results.

The accuracy of the results obtained by the integral equation approach may possibly be improved by improving upon the functional relationship between the velocity on the body surface and the velocity above the body surface. Again an examination of the boundary condition shows that it needs an improvement. The exact boundary condition on the body surface can be written as

$$\lim_{r \rightarrow 0} \phi_r = (1 + \phi_x) \frac{dR}{dx}$$

In the accelerating transonic flow it is seen that ϕ_x is of the same order of magnitude as compared to unity and the nonlinear term $\phi_x \phi_{xx}$ is retained in the transonic flow equation. Hence it appears that it is appropriate to retain term like $\phi_x \frac{dR}{dx}$ in the boundary condition, and the problem should be solved accordingly.

REFERENCES

1. Ashley, H. and Landahl, M. (1965), "Aerodynamics of Wings and bodies ", Addison-Wesley publishing Company, Inc. Reading, Massachusetts.
2. Bailey, F.R.(1971), "Numerical calculation of transonic flow about slender bodies of revolution", NASA TN-D 6582.
3. Carnahan Brice, Luther, H.A.(1969), Wilkes James O., "Applied Numerical Methods ", John Wiley and Sons.,Inc.
4. Cole, J.D. and Messiter, A.F.(1957), "Expansion procedures and similarity laws for transonic flow", ZAMP, Vol.8, pp. 1-25.
5. Fink, M.R.(1971), "Calculated transonic flow past slender fuselages and afterbodies" , Jour. of Aircraft, Vol.8, No.9, pp.710.
6. Guderley, K.G. (1950), "Axial symmetric flow patterns at a free stream Mach number close to one ", USAF. Tech. Report 6285.
7. Gradshteyn, I.S. and Ryzhik, I.M. (1965), "Tables of integrals, series and products", Academic Press.
8. Heaslet, M.A. and Spreiter, J.R. (1956), "Three dimensional transonic flow theory applied to slender wings and bodies", NACA Tech. Rept. 1318 (Also NACA TN 3717).
9. Heaslet, M.A., Lomax, H. and Spreiter, J.R. (1950), "Linearized compressible flow theory for sonic flight speeds", NACA Rep. No. 956.
10. Hosokawa, I. (1959), "A refinement of the linearized transonic flow theory", Jour. of Phy. Soc. of Japan, Vol. 15, No. 1, pp. 149.
11. Hosokawa, I. (1962), "A simplified analysis for transonic flows around thin bodies", Symposium transsonicum, AACHEN, Edited by Oswatitsch.

23. Spreiter, J.R. and Stahara, S.S.(1971), "Aerodynamics of slender bodies and wingbody combinations at $M_\infty = 1$ ", AIAA Jour. Vol.9, No.9, pp 1784.
24. Spreiter, J.R. and Stahara, S.S. (1971), "Calculative techniques for transonic flows about certain classes of airfoils and slender bodies", NASA CR-1722.
25. Taylor, R.A. and Mc Devitt, J.B. (1958), "Pressure distributions at transonic speeds for parabolic arc bodies of revolution having fineness ratios of 10, 12 and 14 ", NACA TN 4234.
26. Ward, G.N. (1949), "Supersonic flow past slender pointed bodies", Quar. Jour. Mech. and Appl. Math. Vol.2, pp. 75-97.
27. Ward, G.N. (1955), "Linearized theory of steady high speed flow", Cambridge University Press.

APPENDIX A

ASYMPTOTIC BEHAVIOUR OF ϕ_1 , AS $r \rightarrow 0$

The perturbation equation for transonic flow [equation (2.22)] can be written as

$$\phi_{1rr} + \frac{1}{r} \phi_{1r} = [(\gamma+1) \phi_{1x} - K \phi_{1xx}] \quad (\text{A.1})$$

together with

$$\phi_{1r} \rightarrow \frac{F(x)}{r} \quad \text{as } r \rightarrow 0 \quad (\text{A.2})$$

where $F(x) = R(x) R'(x)$ is the source strength. From (A.2), we can express the expansion of ϕ_1 near $r = 0$, in the form

$$\phi_1 = F(x) \ln r + g_1(x) + \dots \quad (\text{A.3})$$

The first two terms of the expansion are the solution to equation (A.1) with the R.H.S. equal to zero. $F(x)$ is known but $g_1(x)$ is an unknown function of x . The successive terms in the expansion can be obtained by iteration. Thus using the first term in (A.3) i.e. $\phi_1 = F(x) \ln r$ in the R.H.S. of equation (A.1), we obtain

$$\begin{aligned} \phi_{1rr} + \frac{1}{r} \phi_{1r} &= [(\gamma+1) F'(x) \ln r - K] F'' \ln r \\ &= (\gamma+1) F' F'' (\ln r)^2 - K F'' \ln r \end{aligned} \quad (\text{A.4})$$

This admits solution of the form

$$\begin{aligned}\phi_1(x, r; K) &= F(x) \ln r + g_1(x, K) + (r^2 \log^2 r) \\ &= \left(\frac{\gamma+1}{4} F' F''\right) + O(r^2 \log r)\end{aligned}\tag{A.5}$$

Thus

$$\phi_{1r} = \frac{F(x)}{r} + O(r^2 \ln^2 r)\tag{A.6}$$

APPENDIX BSIMPLIFICATION OF THE INTEGRAL TERM IN EQUATION (3.27)

$$I = \int_{-\infty}^{\infty} \frac{\bar{u}^2(\xi, 0)}{2b} E(|\bar{x} - \xi|; b) d\xi \quad (B.1)$$

$$\text{where } E(|\bar{x} - \xi|; b) = b \frac{\partial^2}{\partial \xi^2} \left(\int_0^{\infty} \frac{e^{-\rho^2/b}}{\sqrt{(\bar{x} - \xi)^2 + \rho^2}} d\rho \right) \quad (B.2)$$

Integration in (B.2) can be carried out by using tables of integrals [see. e.g. Gradshteyn and Ryzhik (1965)]. Thus we obtain

$$E(|\bar{x} - \xi|; b) = b \frac{\partial^2}{\partial \xi^2} \left[\frac{\pi}{2} (\bar{x} - \xi) \{ H_1'(Z) - N_1'(Z) \} - (\bar{x} - \xi) \right] \quad (B.3)$$

$$\text{with } Z = \frac{2(\bar{x} - \xi)}{b}.$$

Here H_1 and N_1 are the Struve and Neumann functions of first order respectively. For small Z these functions can be represented in series form as [see e.g. Losch (1960)]

$$H_1(Z) = \frac{2}{\pi} \left[\frac{Z^2}{1 \cdot 3} - \frac{Z^4}{1 \cdot 3 \cdot 5} + \frac{Z^6}{1 \cdot 3 \cdot 5 \cdot 7} - \dots \right]$$

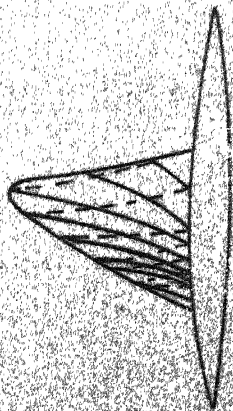
$$N_1(Z) = \frac{2}{\pi} [\ln(Z/2) + C] \left[\frac{Z/2}{1!} - \frac{(Z/2)^3}{1! 2!} + \frac{(Z/2)^5}{2! 3!} - \dots \right] - \frac{2}{\pi Z} \\ - \frac{Z}{2\pi} \left[1 - \frac{(Z/2)^2}{1! 2!} \left\{ 1 + \left(1 + \frac{1}{2}\right) \right\} + \frac{(Z/2)^4}{2! 3!} \left\{ 1 + \frac{1}{2} + \left(1 + \frac{1}{2} + \frac{1}{3}\right) - \dots \right\} \right]$$

After carrying out differentiation in (B.3), we obtain

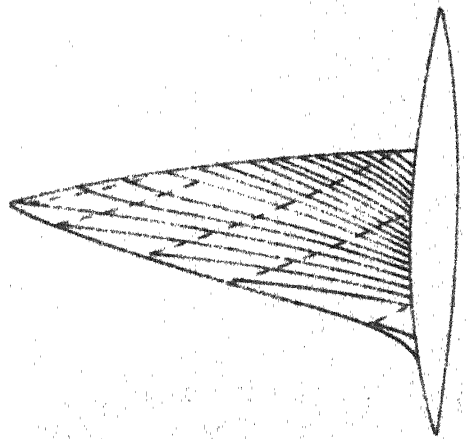
$$E(|\bar{x} - \xi|; b) = b \left\{ -\pi \left(\frac{dZ}{d\xi} - \frac{(\bar{x} - \xi)}{2} \frac{d^2 Z}{d\xi^2} \right) [H_1'(Z) - N_1'(Z)] \right. \\ \left. + \frac{\pi}{2} (\bar{x} - \xi) \left(\frac{dZ}{d\xi} \right)^2 [H_1''(Z) - N_1''(Z)] \right. \\ = b \left\{ \frac{2\pi}{b} \left[1 + \frac{3}{4} Z \frac{db}{d\xi} + Z^2 \left(\frac{db}{d\xi} \right)^2 - \frac{b}{8} Z^2 \frac{d^2 b}{d\xi^2} \right] \right. \\ \left. [H_1'(Z) - N_1'(Z)] + \frac{\pi}{b} Z \left[1 + Z \frac{db}{d\xi} + \frac{Z^2}{4} \left(\frac{db}{d\xi} \right)^2 \right] \right. \\ \left. [H_1''(Z) - N_1''(Z)] \right\} \dots (B.4)$$

Here, assuming that $Z \sim O(1)$ and $\frac{db}{d\xi}$, $\frac{d^2 b}{d\xi^2} < < 1$, we can neglect the terms containing the derivative of b in equation (B.4). Then E is obtained as a function of $Z = \frac{2(\bar{x} - \xi)}{b}$ alone. Thus

$$E(|\bar{x} - \xi|; b) \equiv E(Z) = 2\pi [H_1'(Z) - N_1'(Z)] + \pi Z [H_1''(Z) - N_1''(Z)] \\ = 2\pi \{ [H_1'(Z) - N_1'(Z)] + \frac{Z}{2} [H_1''(Z) - N_1''(Z)] \} \dots (B.5)$$



$M_{\infty} = 0.975$
 $f = 10$



$M_{\infty} = 0.990$
 $f = 10$

FIG.1 SUPERSONIC REGION AND MACH LINES FOR A
 PARABOLIC ARC OF REVOLUTION IN FREE AIR

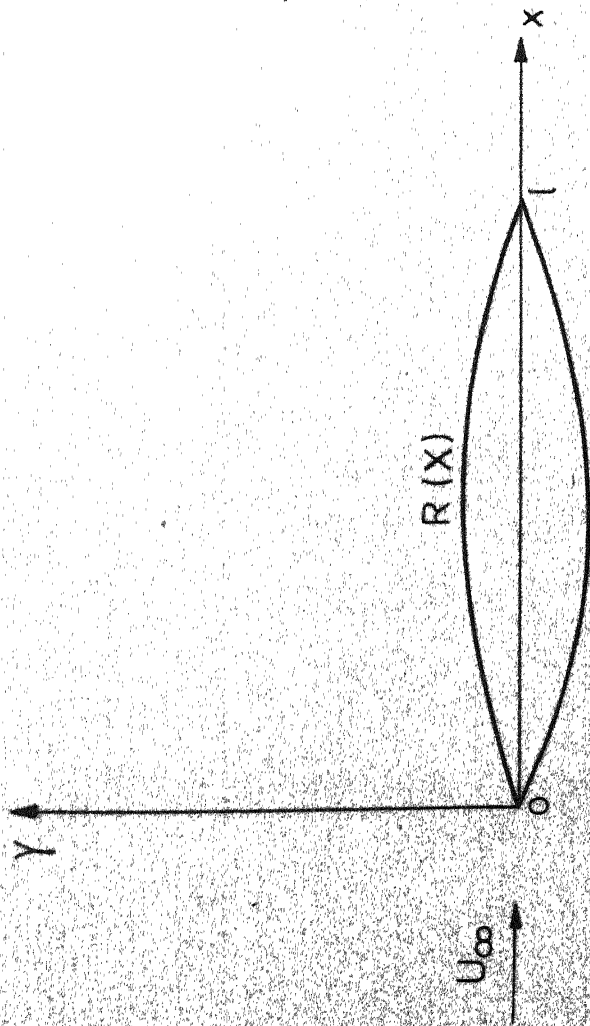


FIG. 2 BODY AND COORDINATE SYSTEM

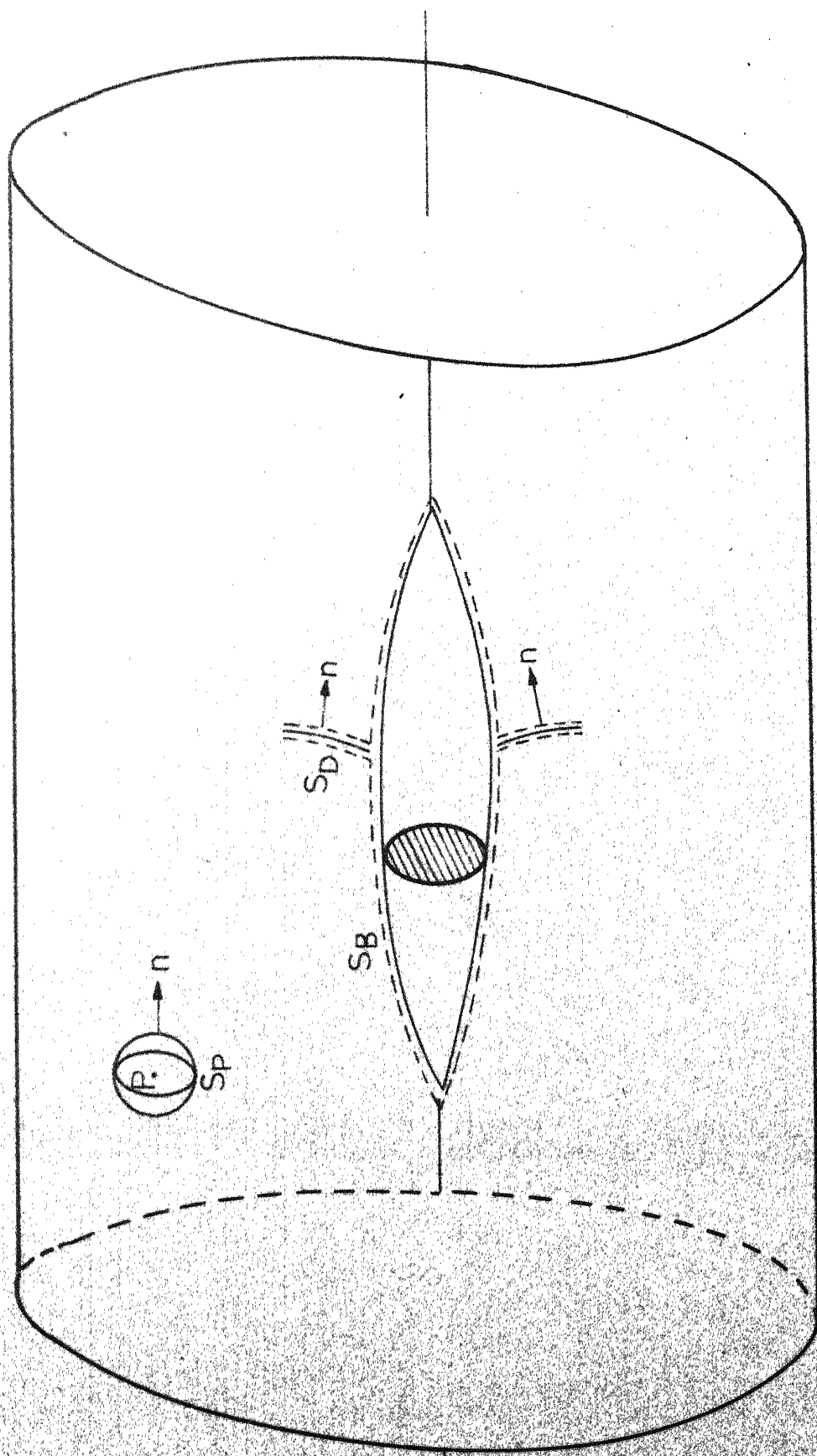


FIG.3 REGION OF INTEGRATION

START

READ M_∞, t, X

CALL LINEAR
CALCULATION OF
LINEAR VELOCITY, \bar{u}_L

$\mu \leftarrow 0$

$u \leftarrow \bar{u}_L$

SOLUTION OF SET OF N
DIFFERENTIAL EQUATIONS

$$\frac{d\bar{u}_R}{d\mu} = f(\bar{u}_1, \bar{u}_2, \dots, \bar{u}_n; \mu)$$

BY HAMMING'S PREDICTOR
CORRECTOR METHOD

CALCULATION OF FINAL
VELOCITY AND PRESSURE
DISTRIBUTION AT $\mu=1$

STOP

IS
 $\mu \cdot u_R \geq 1$

NO

YES

CALL STEEP
SOLUTION OF
ALGEBRAIC
EQUATIONS BY
STEEPEST DESCENT
TECHNIQUE

NO

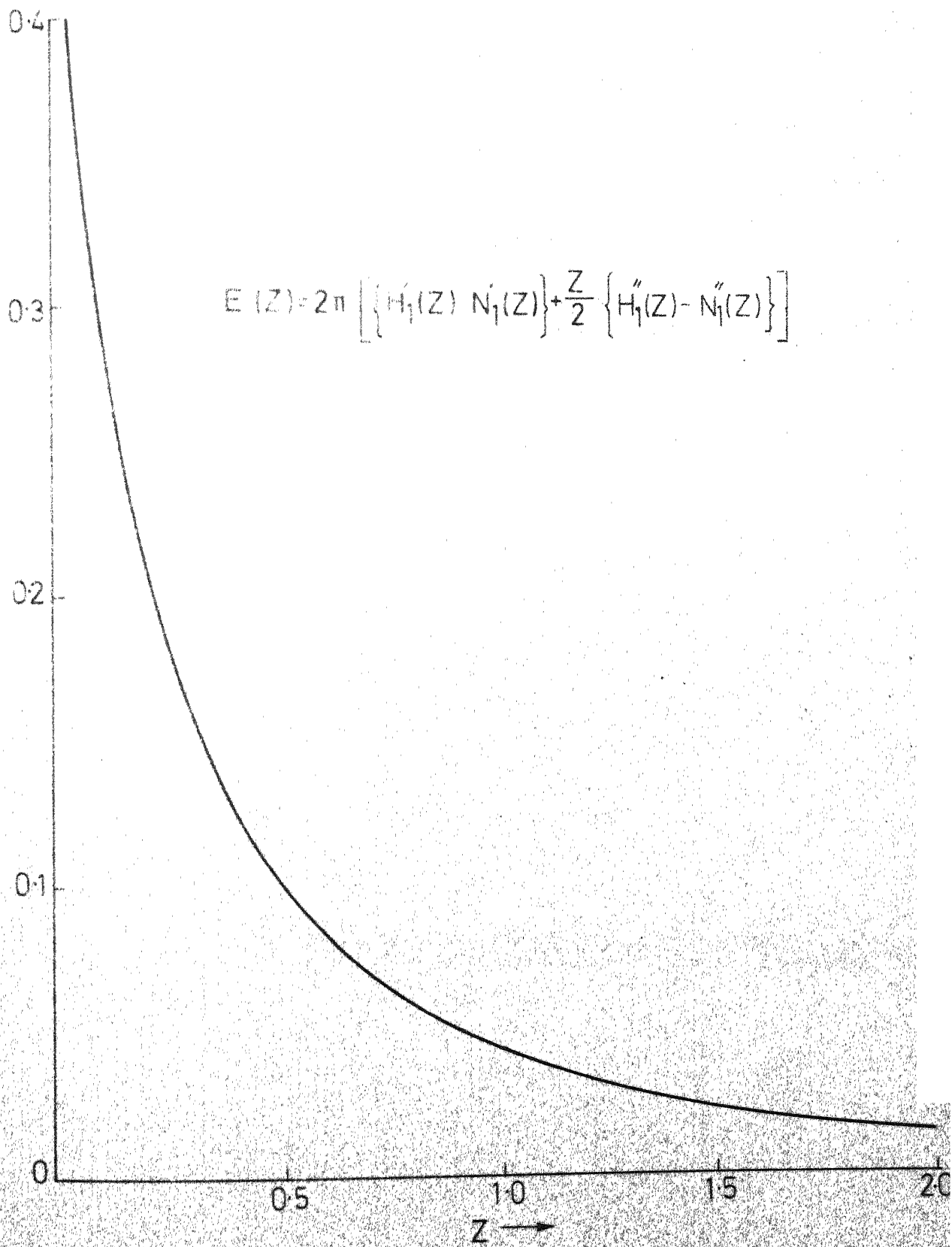
IS
 $\mu=1$

YES

$\mu = \mu + H$

INFLUENCE COEFFICIENT $E(Z)$

$$E(Z) = 2\pi \left[\left\{ H_1'(Z) N_1'(Z) \right\} + \frac{Z}{2} \left\{ H_1''(Z) - N_1''(Z) \right\} \right]$$



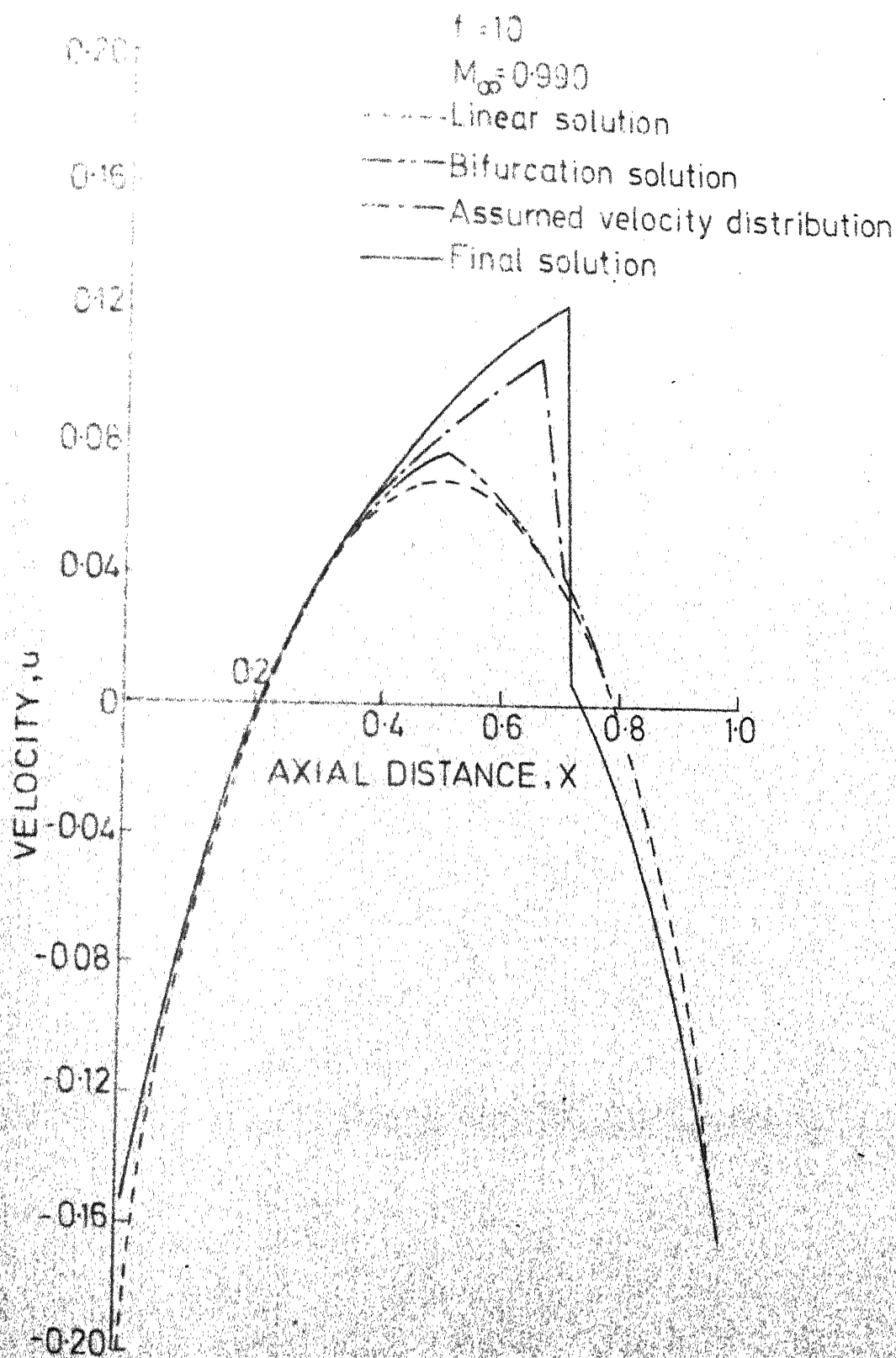


FIG. 6 VELOCITY DISTRIBUTION (DISCONTINUOUS CASE)

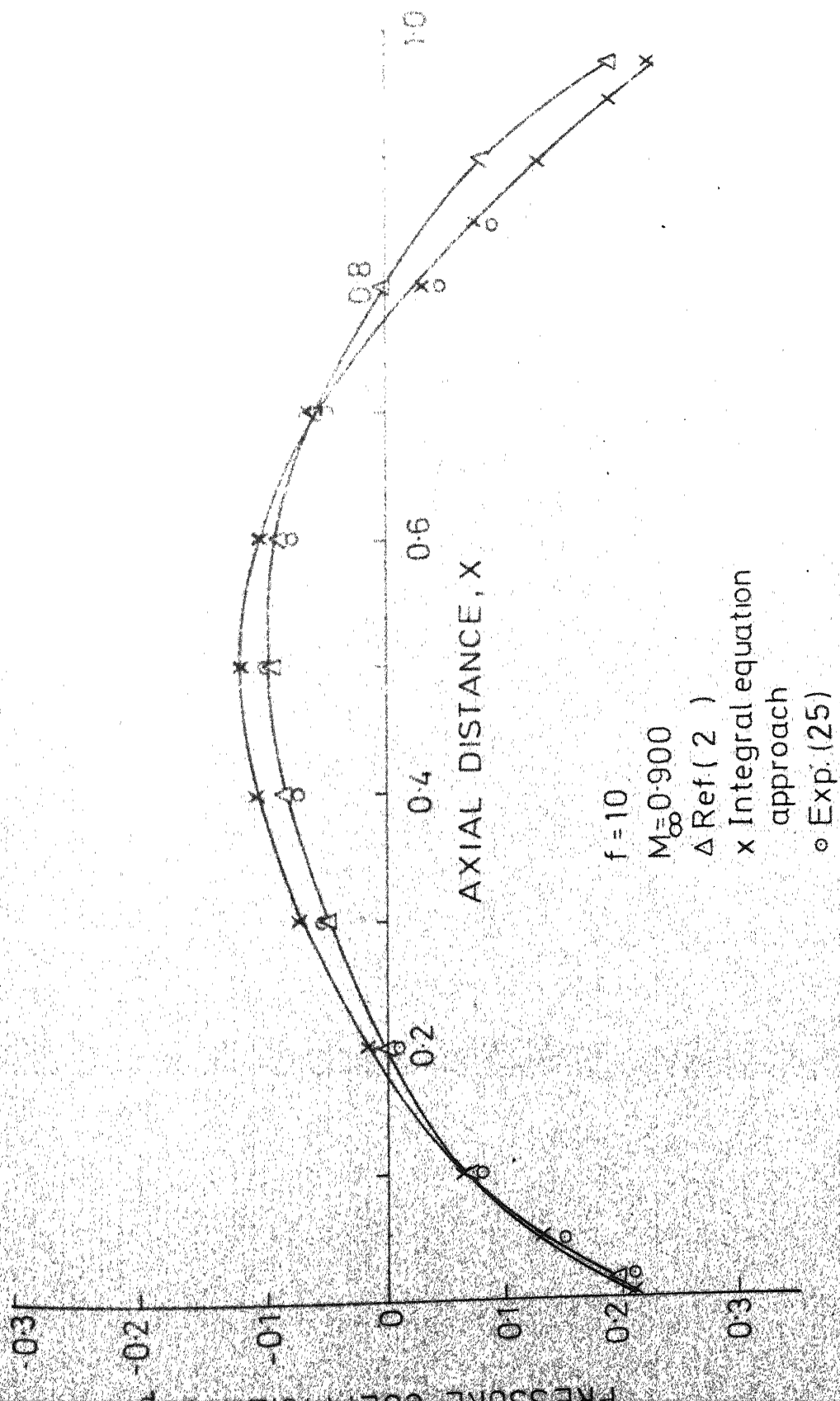


FIG.7 COMPARISON OF PRESSURE DISTRIBUTION (CONTINUOUS CASE)

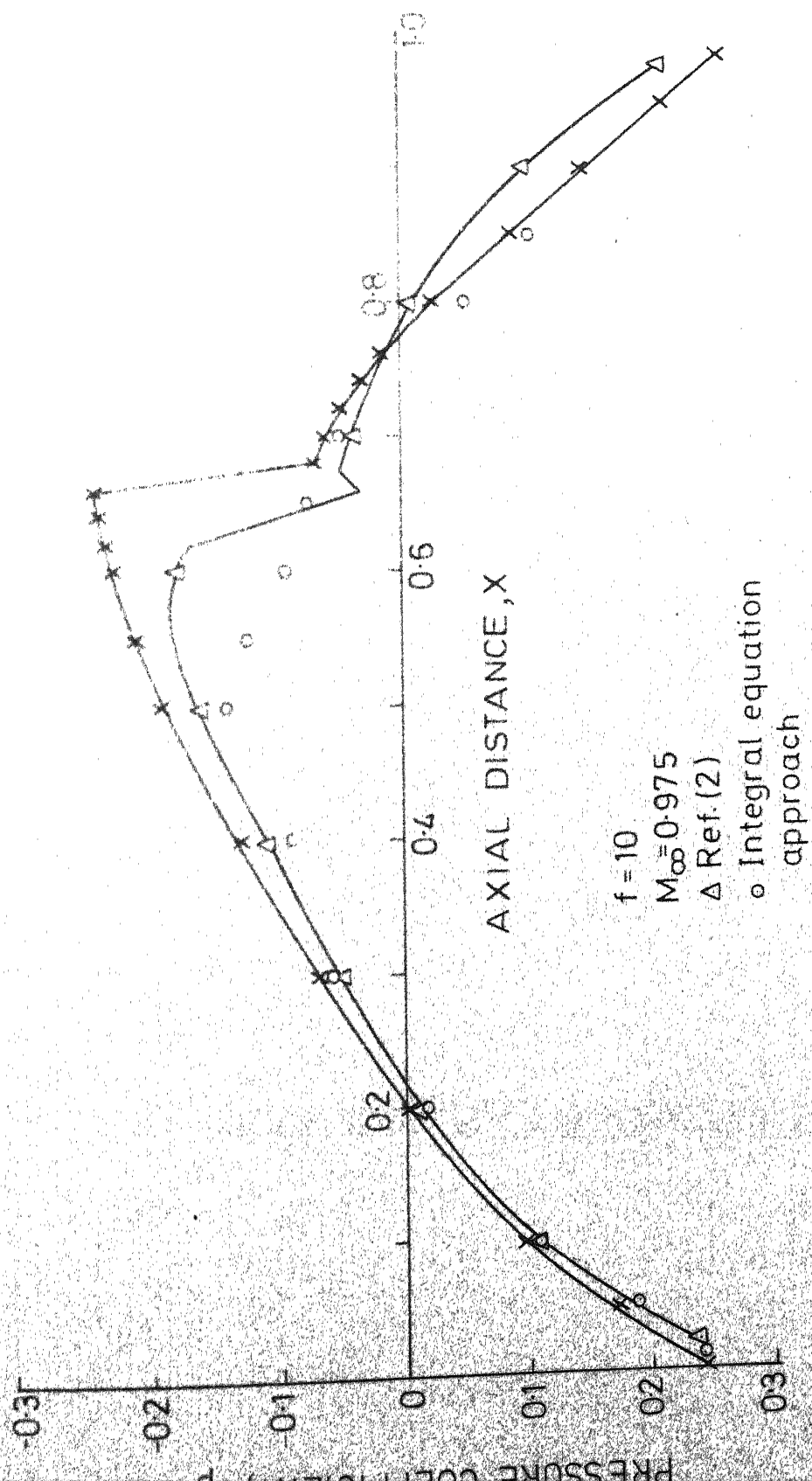


FIG.8 COMPARISON OF PRESSURE DISTRIBUTION (DISCONTINUOUS CASE)

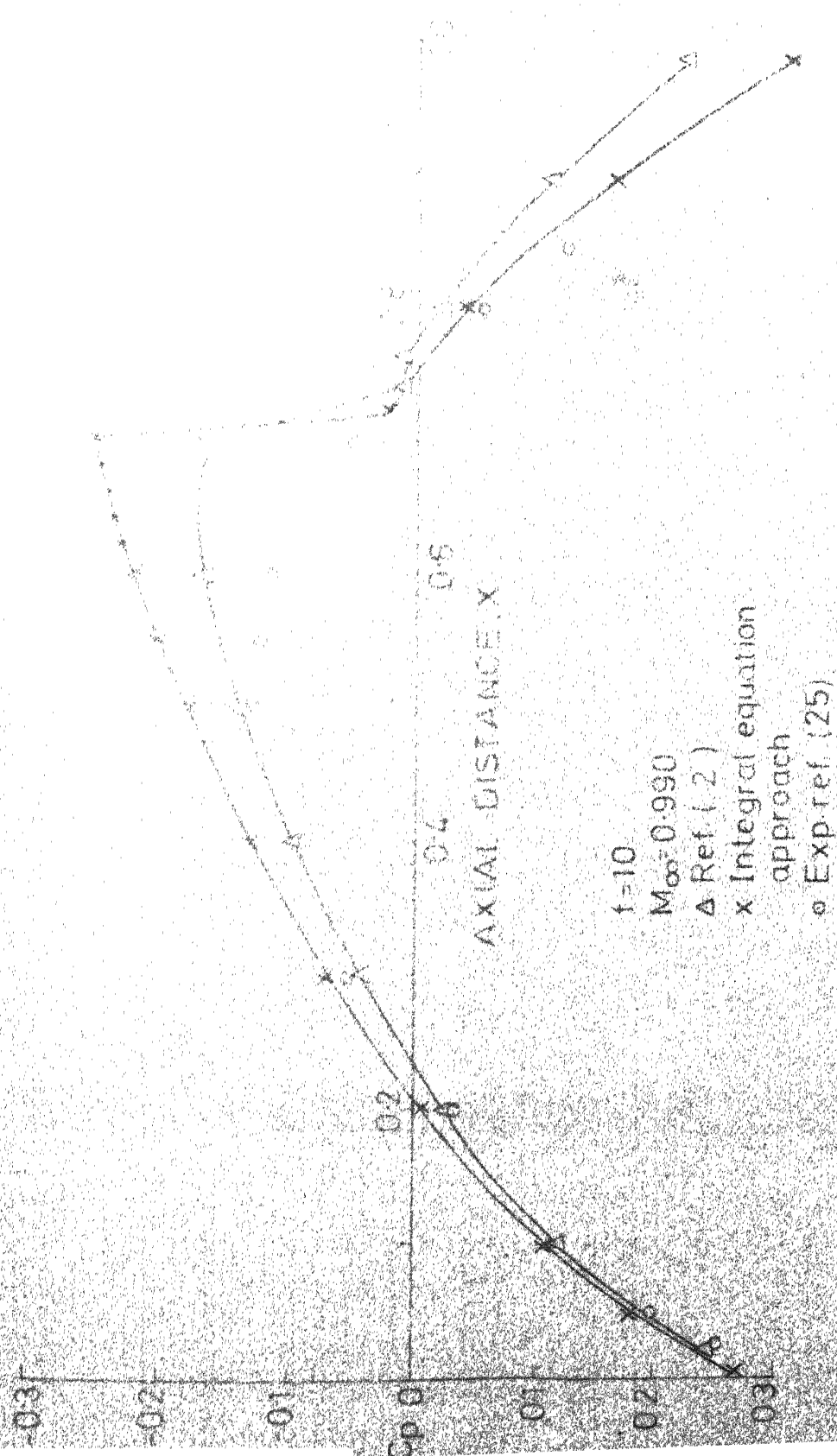


FIG-9 COMPARISON OF PRESSURE DISTRIBUTION (DISCONTINUOUS CASE)

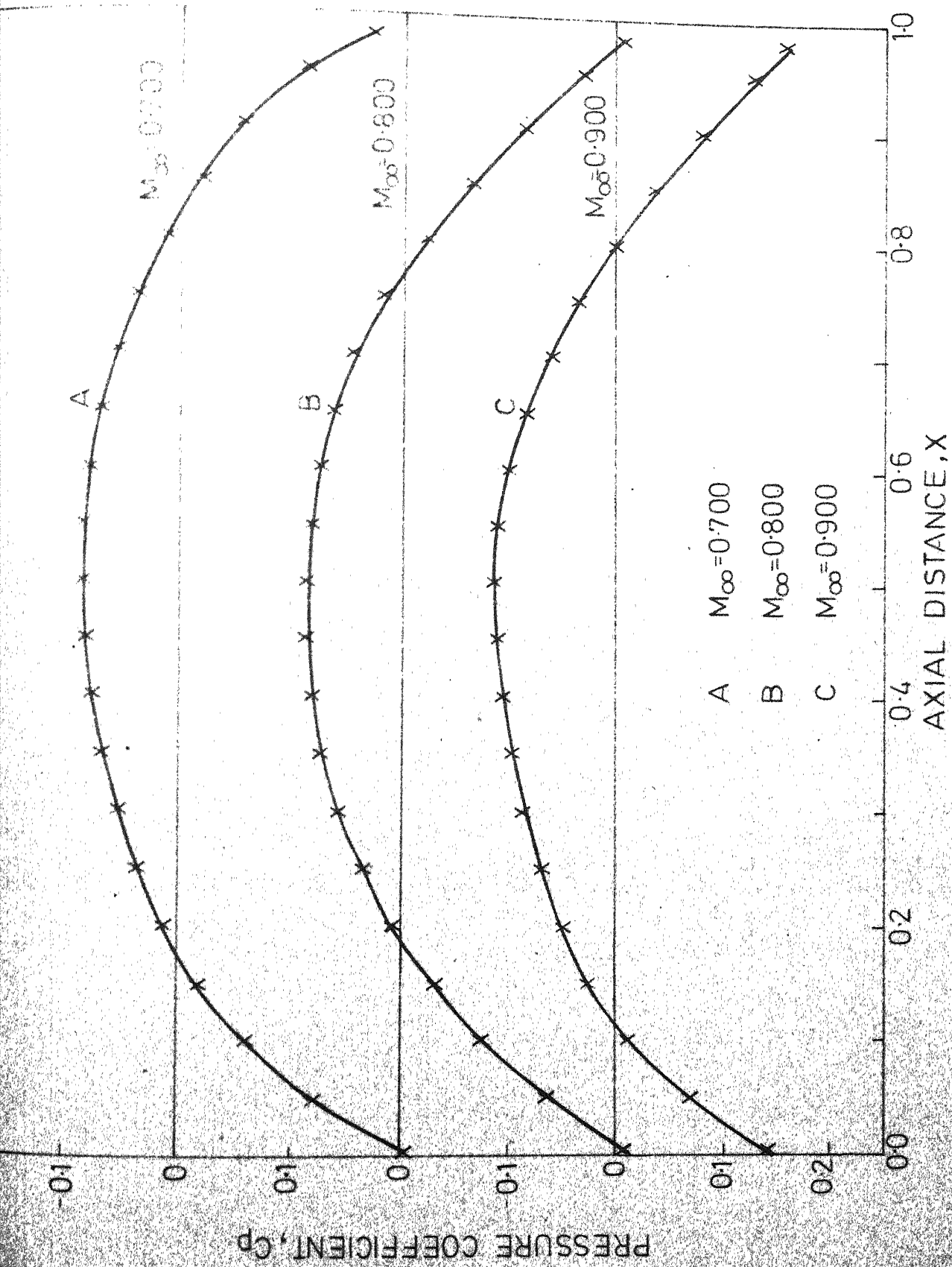


FIG.10 PRESSURE DISTRIBUTION FOR FINENESS RATIO 10 AT DIFFERENT MACH NUMBERS

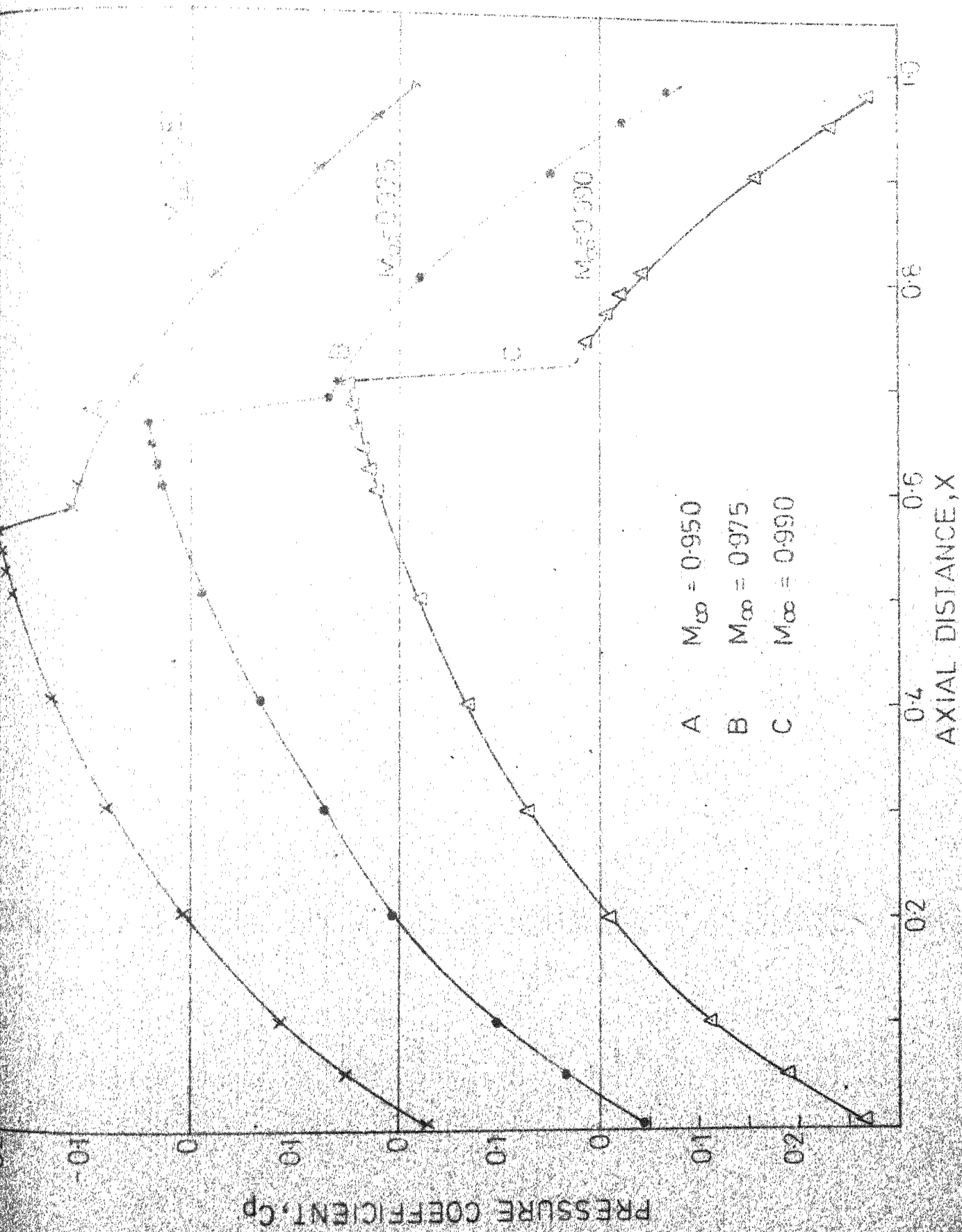


FIG.11 PRESSURE DISTRIBUTION FOR FINENESS RATIO 10 AT VARIOUS

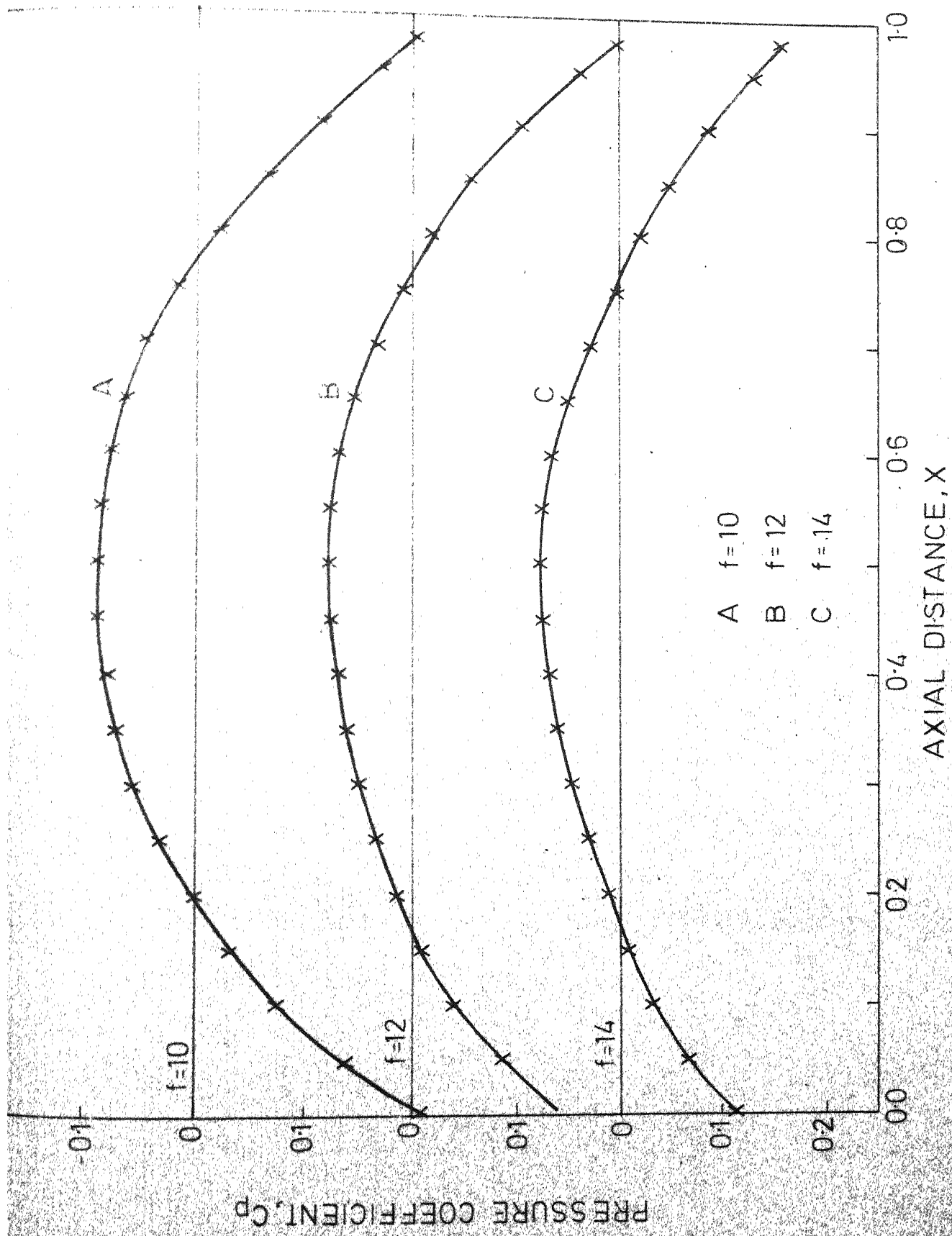


FIG.12 PRESSURE DISTRIBUTION AT $M_\infty=0.800$ FOR DIFFERENT FINENESS RATIOS

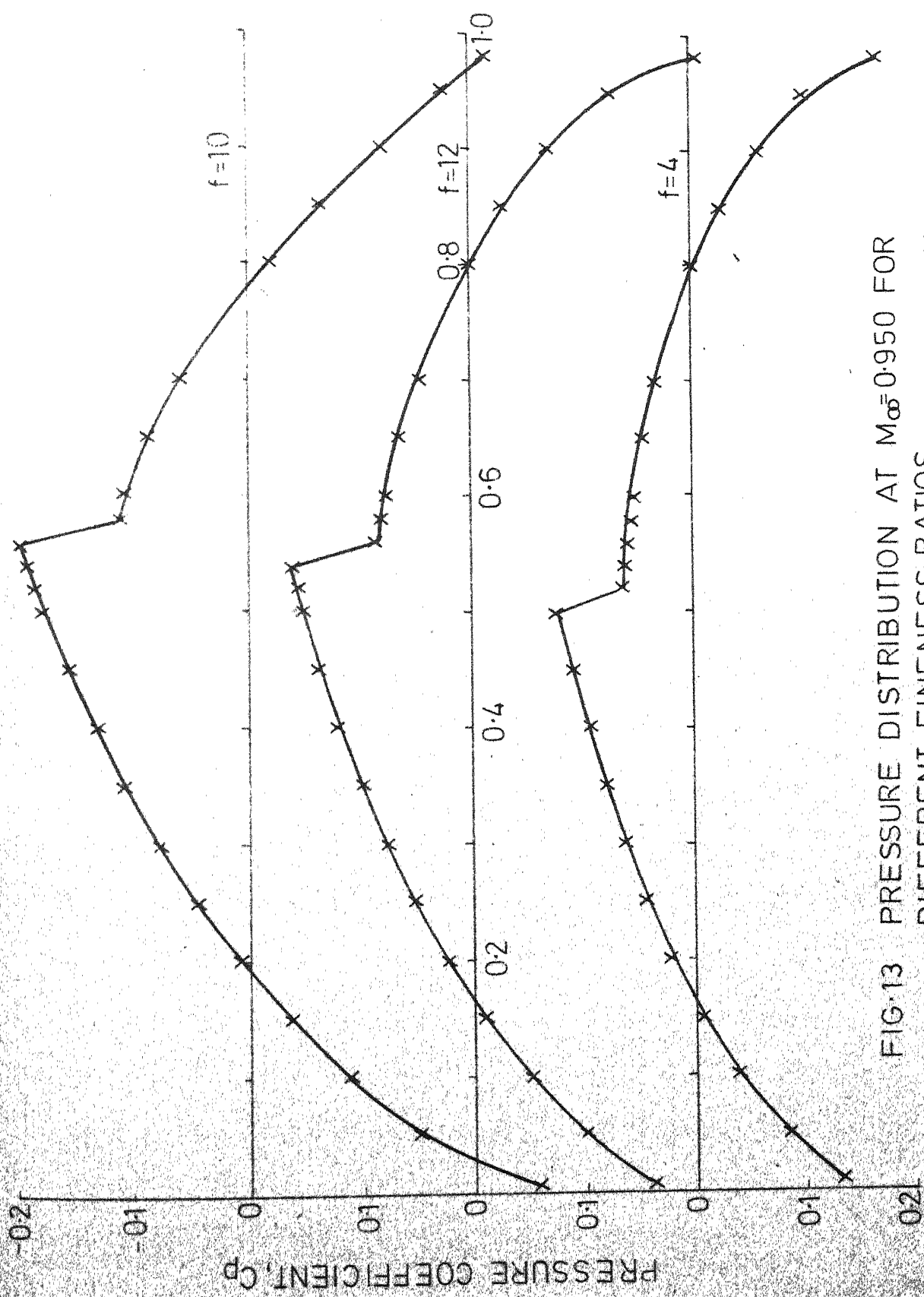


FIG. 13 PRESSURE DISTRIBUTION AT $M_\infty=0.950$ FOR DIFFERENT FINENESS RATIOS

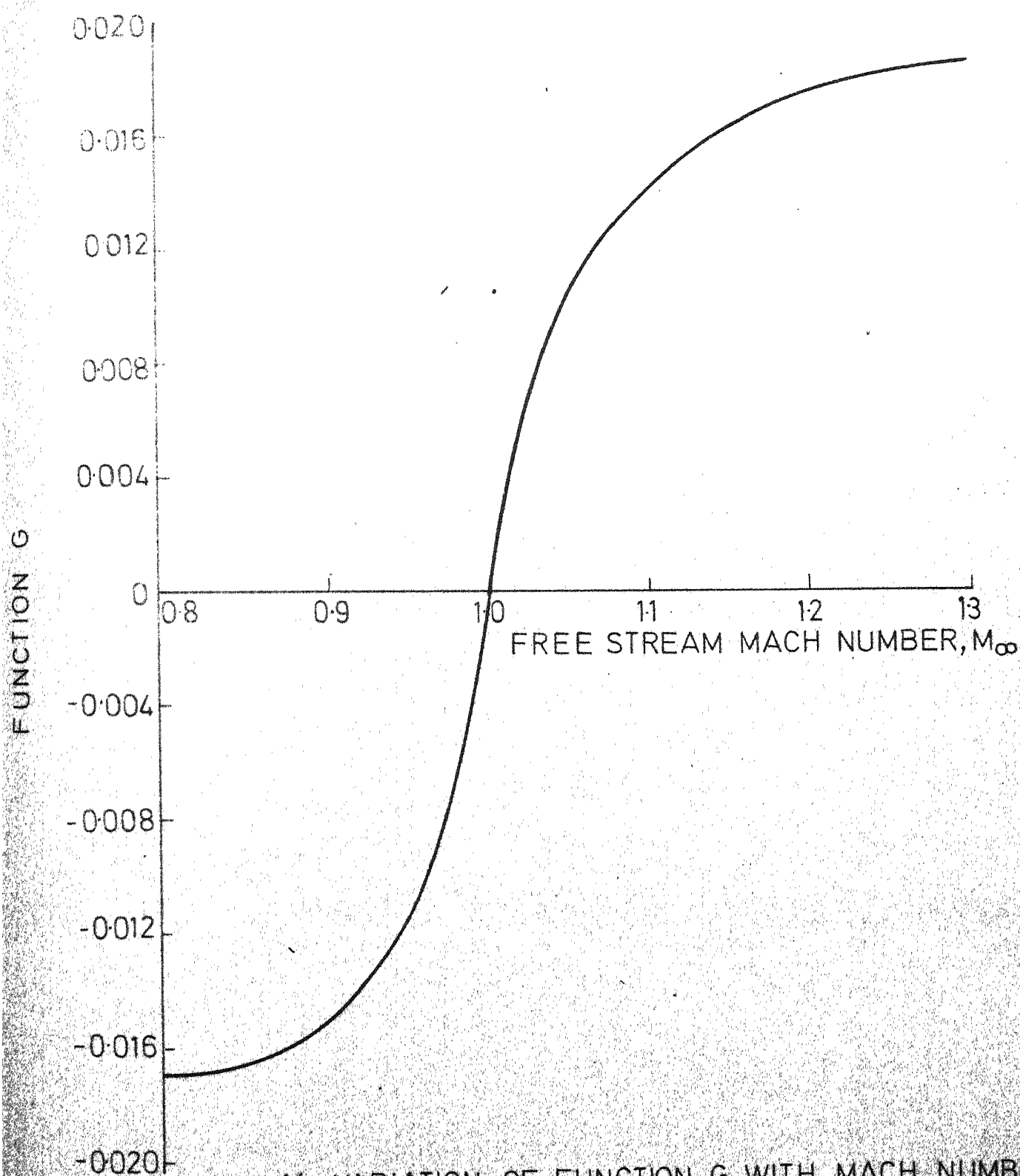


FIG-14 VARIATION OF FUNCTION G WITH MACH NUMBER

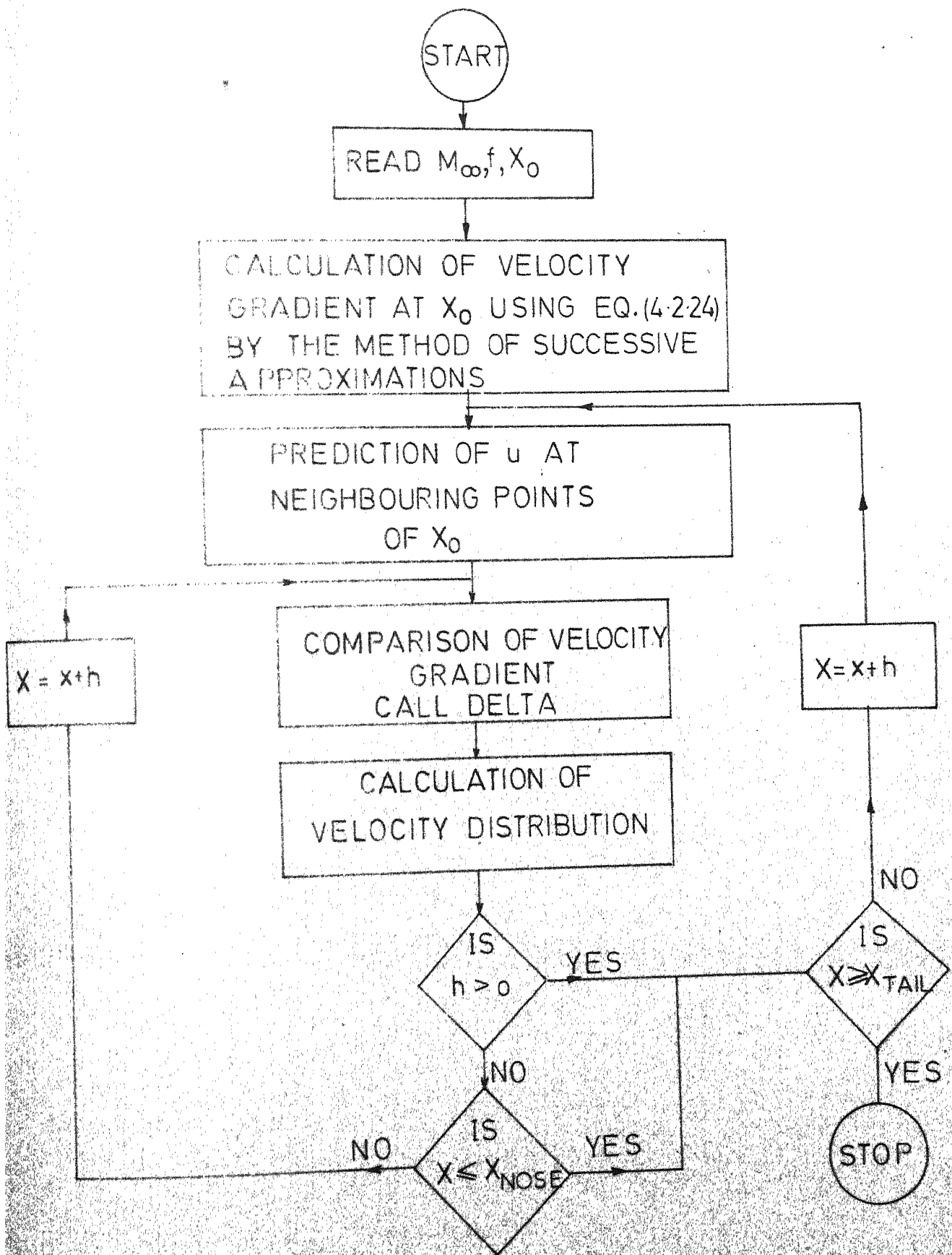


FIG 14a FLOW CHART OF THE COMPUTER PROGRAM FOR THE METHOD OF LOCAL LINEARIZATION

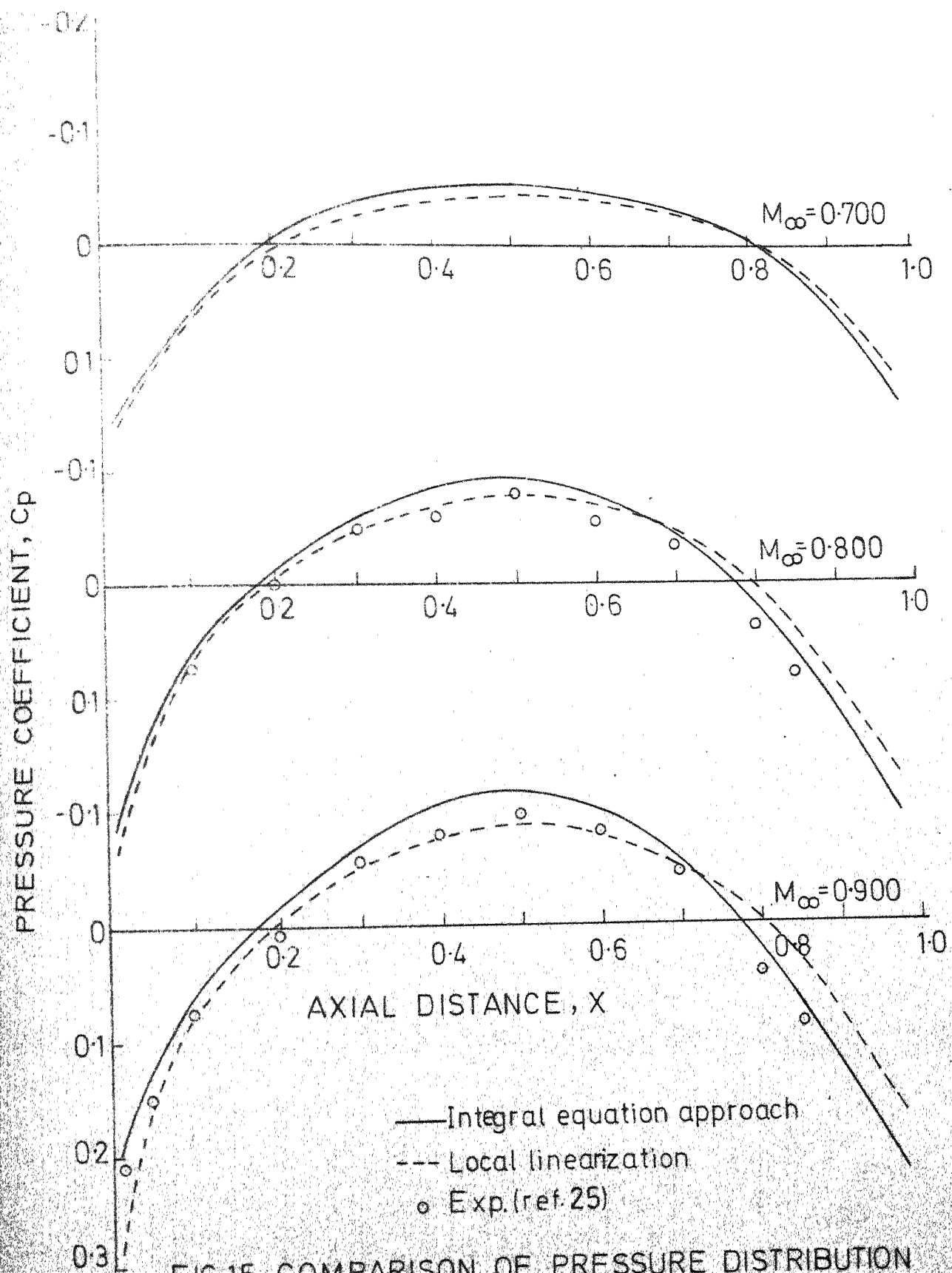


FIG.15. COMPARISON OF PRESSURE DISTRIBUTION
(CONTINUOUS CASE)

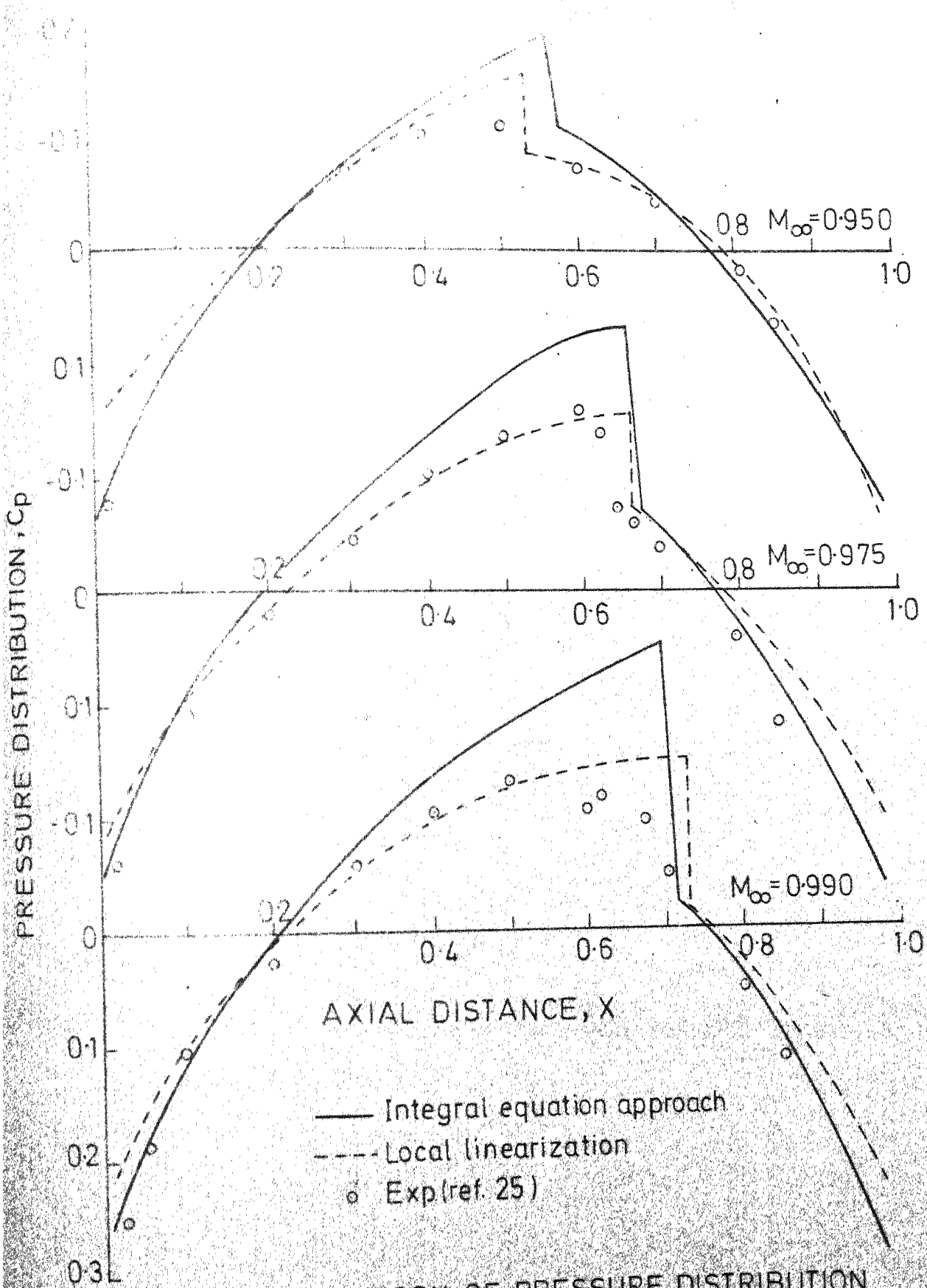


FIG.16 COMPARISON OF PRESSURE DISTRIBUTION (DISCONTINUOUS CASE)

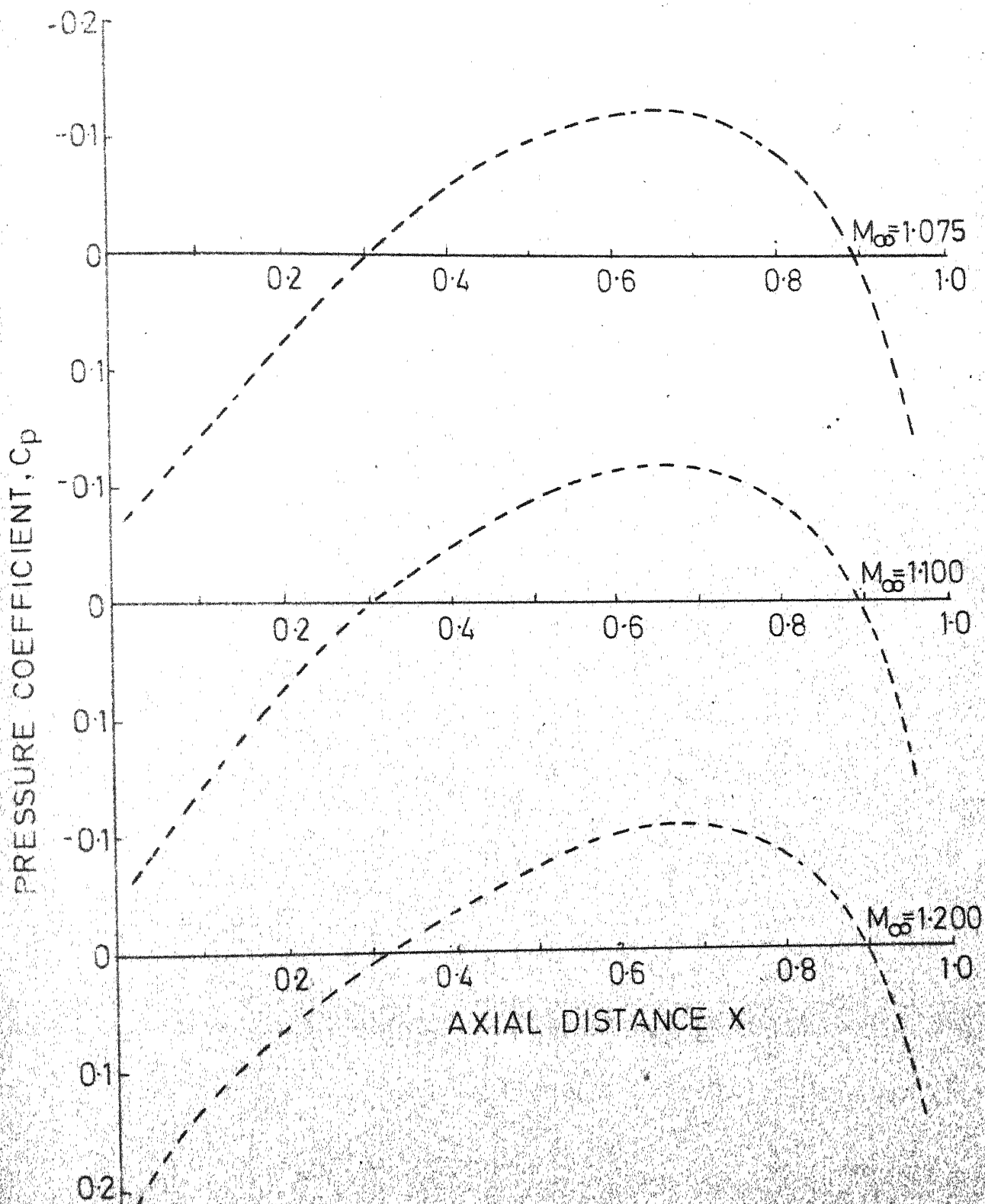


FIG. 17 PRESSURE DISTRIBUTION FOR FINENESS RATIO 10 AT HIGH TRANSONIC SPEEDS BY LOCAL LINEARIZATION METHOD

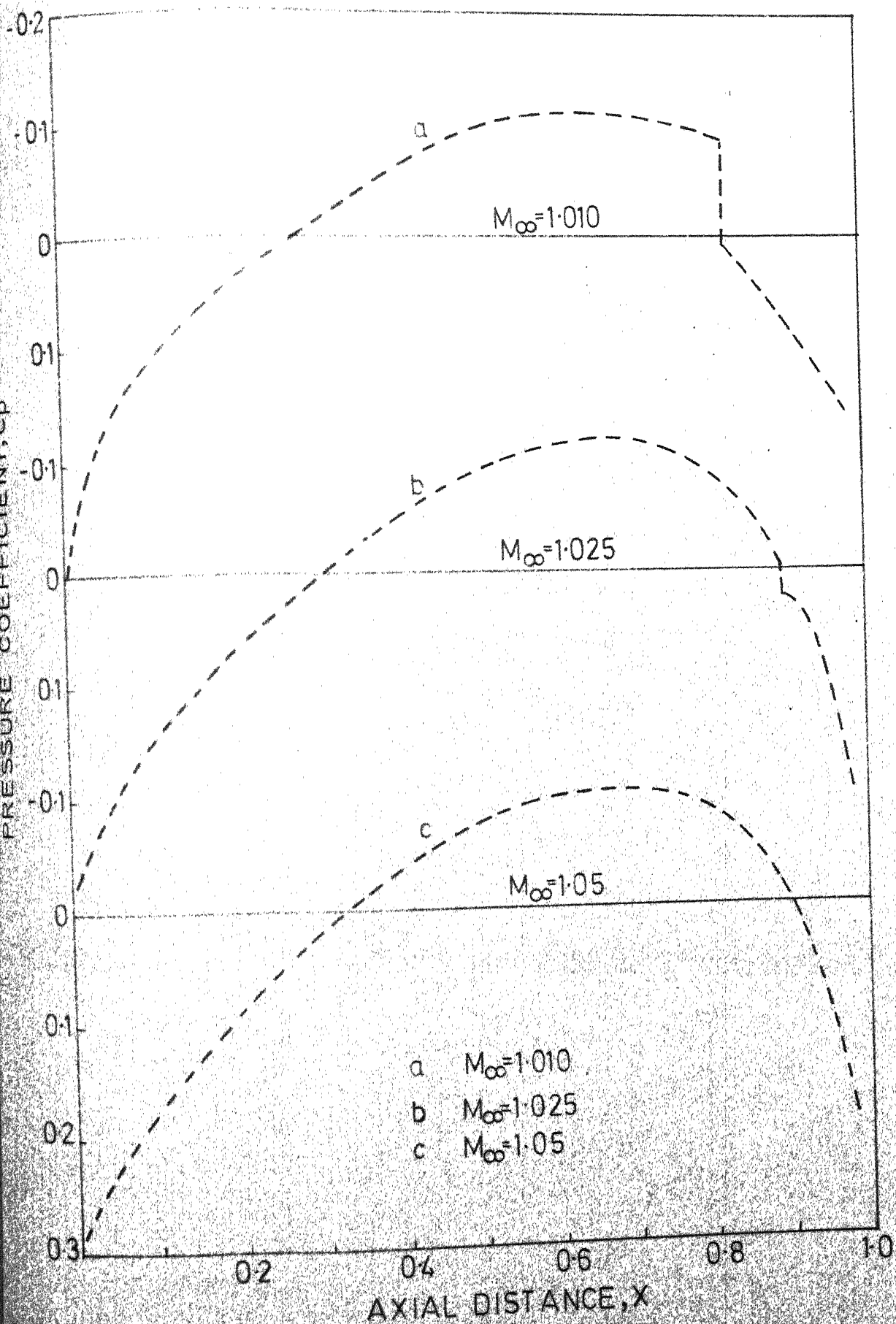


FIG. 18 PRESSURE DISTRIBUTION FOR FINENESS RATIO 10 AT HIGH TRANSONIC SPEEDS BY LOCAL LINEARIZATION METHOD

APPEND C

LISTING OF THE PROGRAM

*IBJDE

*IBFTC MAIN

AMEW ARTIFICIAL VISCOSITY PARAMETER
 CP LINEAR PRESSURE DISTRIBUTION
 CPP FINAL PRESSURE DISTRIBUTION
 F INFLUENCE FUNCTION
 F VELOCITY DERIVATIVE
 FR FINENESS RATIO
 H STEP SIZE
 L LIMITS OF INTEGRATION
 K
 MKR TOTAL NUMBER OF DIFFERENT CASES
 U VELOCITY VECTOR
 UBR LINEAR VELOCITY DISTRIBUTION
 USP PREDICTED SOLUTION
 USN FINAL VELOCITY DISTRIBUTION
 URR VELOCITY DISTRIBUTION ASSUMED AT BIFURCATION POINT
 X POINTS ALONG THE LENGTH OF THE BODY
 YAM MACH NUMBER

INPUT VARIABLES ARE X , YAM , TC , URR

```

25  FORMAT(10X,* YAM =*,F6.3,10X,* FINENESS RATIO=*,I3/)
30  FORMAT(8F7.4)
33  FORMAT(F5.3,I2)
46  FORMAT(5F5.2)
51  FORMAT(1X,I5,7F15.5/)
101 FORMAT(5X,*I*,10X,*X(I)*,11X,*Y(I)*,10X,*YD(I)*,10X,*YDD(I)*,
58X,*UBR(I)*,11X,*R(I)*,11X,*CP(I)*/)
151 FORMAT(2X,16F8.3)
210  FORMAT(1X,I8,3F20.4)
444  FORMAT(2X,16F8.3)
555  FORMAT(2X,130(1H*)/)
556  FORMAT(2X,*NY=*,I3)
680  FORMAT(5F7.4)
757  FORMAT(8F7.3)
2185 FORMAT(2X,*L =*,I3,5X,*AMEW =*,F8.4/)
2785 FORMAT(1X,16F8.4/)

```

DIMENSION X(25),CP(25),Y(25),YD(25),YDD(25),UBR(25),E(25,25),

```

1R(25),U(25,21),UU(25),F(25,21),PHI(25),CPP(25),Z2(25),USL(25,21)
2USP(25,21),US(25,21),USN(25,21),FS(25,21),UST(25,21),FSH(25,21),
3URR(25)

```

```

COMMON/SET7/YAM,PAI,TC

```

```

COMMON/SET8/UBR,AMEW

```

```

COMMON/SET1/X,N,NN

```

```

COMMON/SET9/NVK

```

```

INTEGER FR

```

```

MKR=10

```

```

N=20

```

```

NN=N-1

```

```

C
C
C
EXPRESSION FOR PARABOLIC ARC PROFILE

```

```

YP(A)=(TC/2.)*(1.-(2.*A-1.))**2)

```

```

READ 30,(X(I),I=1,N)

```

```

DO 4 II=1,MKR

```

```

IF(MKR.GE.6) READ 31,(X(IL),IL=1,N)

```

```

READ 33,YAM,FR

```

```

TC=1.0/FLOAT(FR)

```

```

PAI=4.0*ATAN(1.0)

```

```

PRINT 555

```

```

PRINT 25,YAM,FR

```

```

PRINT 556

```

```

C
C
C
CALCULATION OF LINEAR VELOCITY AND PRESSURE DISTRIBUTION

```

```

PRINT 1:

```

```

CALL LINEAR(UBR)

```

```

DO 10 I=1,N

```

```

IF(X(I).EQ.0.) GO TO 10

```

```

A=X(I)

```

```

15 Y(I)=(TC/2.)*(1.-(2.*A-1.))**2)

```

```

YD(I)=2.*TC*(1.-2.*A)

```

```

YDD(I)=-4.*TC

```

```

16 R(I)=ABS(UBR(I)/YDD(I))

```

```

C4=(1.-YAM*YAM)/(2.4*YAM*YAM)

```

```

UBR(I)=UBR(I)*C4

```

```

CP(I)=-2.*UBR(I)-4.*TC*TC*((1.-2.*X(I))**2)

```

```

PRINT 60,I,X(I),Y(I),YD(I),YDD(I),UBR(I),R(I),CP(I)

```

```

UBR(I)=UBR(I)/C4

```

```

17 CONTINUE

```

```

C
C
C
INITIAL CONDITIONS

```

```

690 H=0.05

```

```

AMEW=0.0

```

```

NVK=1

```

```

DO 85 J=2,N

```

```

U(J,1)=UBR(J)

```

```

US(J,1)=U(J,1)

```

55 CONTINUE

K1=4

K2=2

RUNGE KUTTA METHOD

DO 110 L=1,4

CALL DERIV(F,U,AMEW,E,L)

IF(L.EQ.1) GO TO 91

DO 92 J=2,N

92 FS(J,L)=F(J,L)

IF(L.EQ.4) GO TO 115

91 DO 87 J=2,N

PHI(J)=F(J,L)

UU(J)=U(J,L)

U(J,L)=UU(J)+0.5*H*F(J,L)

87 CONTINUE

AMEW=AMEW+H*0.5

NVK=2

CALL DERIV(F,U,AMEW,E,L)

DO 90 J=2,N

PHI(J)=2.*F(J,L)+PHI(J)

U(J,L)=UU(J)+0.5*H*F(J,L)

9 CONTINUE

CALL DERIV(F,U,AMEW,E,L)

DO 95 J=2,N

PHI(J)=PHI(J)+2.*F(J,L)

U(J,L)=UU(J)+H*F(J,L)

95 CONTINUE

AMEW=AMEW+H*0.5

CALL DERIV(F,U,AMEW,E,L)

DO 120 J=2,N

PHI(J)=(PHI(J)+F(J,L))/6.

U(J,L+1)=UU(J)+H*PHI(J)

US(J,L+1)=U(J,L+1)

USN(J,L+1)=U(J,L+1)

12 CONTINUE

DO 121 J=2,N

F(J,L+1)=F(J,L)

121 CONTINUE

PRINT 555

PRINT 2185,L,AMEW

PRINT 444,(U(J,L+1),J=2,N)

115 CONTINUE

HAMMINGS PREDICTOR-CORRECTOR METHOD

1215 DO 101 L=K1,K2

AMEW=AMEW+H

LA=L+1

IF(L.GE.8) GO TO 122

```

DO 102 J=2,N
US(J,L+1)=US(J,L-3)+4.*H*(2.*FS(J,L)-FS(J,L-2)+2.*FS(J,L-2))/2.
USP(J,L+1)=US(J,L+1)
IF(L.NE.4) GO TO 12
FS(J,L+1)=FS(J,L)

```

```

1 1 CONTINUE

```

```

GO TO 124

```

```

122 DO 132 J=2,N

```

```

US(J,L+1)=USN(J,L-3)+4.*H*(2.*FS(J,L)-FS(J,L-1)+2.*FS(J,L-2))/2.

```

```

122 USP(J,L+1)=US(J,L+1)

```

```

124 NZ=1

```

```

NY=1

```

```

111 IF(L.EQ.4) GO TO 103

```

```

C UST - MODIFICATION OF PREDICTED VALUE

```

```

DO 104 J=2,N

```

```

104 UST(J,L+1)=USP(J,L+1)+112./121.*(US(J,L)-USP(J,L))

```

```

1030 IF(NZ.EQ.1) GO TO 106

```

```

LA=L+1

```

```

CALL DERIV(FS,US,AMEW,E,LA)

```

```

DO 1060 J=2,N

```

```

C APPLICATION OF HAMMINGS CORRECTOR

```

```

US(J,L+1)=(9.*US(J,L)-US(J,L-2)+3.*H*(FS(J,L+1)+2.*FS(J,L)-FS(J,
51)))/8.

```

```

1061 CONTINUE

```

```

GO TO 107

```

```

106 DO 660 J=2,N

```

```

660 FS(J,L+1)=FS(J,L)

```

```

CALL DERIV(FS,UST,,AMEW,E,LA)

```

```

DO 109 J=2,N

```

```

US(J,L+1)=0.125*(9.*US(J,L)-US(J,L-2)+3.*H*(FS(J,L+1)+2.*FS(J,L)
5FS(J,L-1)))

```

```

109 USL(J,L+1)=US(J,L+1)

```

```

NZ=NZ+1

```

```

GO TO 111

```

```

1 3 LA=L+1

```

```

CALL DERIV(FS,US,AMEW,E,LA)

```

```

DO 103 J=2,N

```

```

103 US(J,L+1)=0.125*(9.*US(J,L)-US(J,L-2)+3.*H*(FS(J,L+1)+2.*FS(J,L)
5-FS(J,L-1)))

```

```

107 CONTINUE

```

```

IF(NZ.EQ.1) GO TO 114

```

```

C APPLICATION OF CONVERGENCE TEST

```

```

DO 108 J=2,N

```

```

108 IF(ABS(1.-(USL(J,L+1)/US(J,L+1))).LT.0.0001) GO TO 118

```

```

PRINT 2185,L,AMEW

```



```

      NY=NY+1
      IF(NY.GT.2) GO TO 118
      JZ=1

```

```

C
C   CHECK FOR THE JACOBIAN MATRI
C

```

```

      DO 13 J=2,N
      XYZ=AMEW*USN(J,L)
      IF(XYZ.GE.1.) JZ=JZ+1
13   CONTINUE
      IF(JZ.GE.2) GO TO 9
      GO TO 114
      9   L1=L
      AMEW=AMEW+H
      PRINT 2185,L1,AMEW
369   READ 757,(URR(J),J=2,N)
      PRINT 555
      PRINT 2785,(URR(J),J=2,N)
      PRINT 555
      DO 361 J=2,N
361   URR(J)=URR(J)/C4
      DO 775 J=2,N
      USN(J,L1)=URR(J)
775   CONTINUE
      27   AMEW=AMEW+H

```

```

C
C   STEEPEST DESCENT CALCULATION TECHNIQUE
C

```

```

      CALL STEEP(USN,L1)
      AMEWI=1./AMEW
      PRINT 2785,(USN(J,L1+1),J=2,N)
      PRINT 2185,L1,AMEW
      L1=L1+1
      IF(L1.LE.20) GO TO 27
      GO TO 820
114   DO 116 J=2,N
116   USL(J,L+1)=US(J,L+1)
      NZ=NZ+1
      GO TO 1030

```

```

C
C   CHECK FOR THE JACOBIAN MATRI
C

```

```

118   DO 970 J=2,N
      XK=AMEW*USN(J,L)
      IF(XK.GE.1.) GO TO 9

```

```

C
C   CALCULATION OF FINAL VELOCITY DISTRIBUTION USN
C

```

```

123   USN(J,L+1)=US(J,L+1)-9./121.*(US(J,L+1)-USP(J,L+1))
      FS(J,L+1)=FS(J,L)
970   CONTINUE

```



```

      K1=K+1
      IF(L.EQ.1.AND.NVK.EQ.1) GO TO 111
      IF(L.NE.1) GO TO 820
      IA=1
      GO TO 830
C2    IA=L
      SUM=SUM+.25*E(J,K)*((U(K,IA)+U(K1,IA))**2/4+.5*AMEW*
      5(U(K,IA)+U(K1,IA))*(F(K,IA)+F(K1,IA)))
      GO TO 20
710   IA=L
      SUM=SUM+.25*E(J,K)*(U(K,IA)+U(K1,IA))**2/4
20    CONTINUE
      F(J,L)=(1./(1.-AMEW*U(J,IA)))*( .5*U(J,IA)*U(J,IA)+SUM)
1     CONTINUE
      RETURN
      END

```

```

C
C
C
*IBFTC SUB2

```

THIS SUBROUTINE CALCULATES THE INFLUENCE COEFFICIENT

ϵ - INFLUENCE COEFFICIENT

```

SUBROUTINE INCOEF(U,U,L)
DIMENSION X(25),E(25,25),R(25),Z2(25),U(25,21)
COMMON/SET7/YAM,PAI,TC
COMMON/SET1/X,N,NN
COMMON/GRP1/R
C4=(1.-YAM*YAM)/(2.4*YAM*YAM)
YP3=.4.*TC
DO 210 JK=2,N
DO 210 KK=2,NN
K1=KK+1
Z2(KK)=(X(K1)+X(KK))*0.5
Z1=Z2(KK)
R(KK)=ABS((U(KK,L)+U(K1,L))/(2.*YP3))
R(KK)=R(KK)*C4
Z=2.*ABS(X(JK)-Z2(KK))/R(KK)

```

```

FDH1Z DENOTES FIRST DERIVATIVE OF STRUVE FUNCTION.
FDY1Z DENOTES FIRST DERIVATIVE OF NEUMANN FUNCTION.
SDY1Z DENOTES SECOND DERIVATIVE OF NEUMANN FUNCTION.
SDH1Z DENOTES SECOND DERIVATIVE OF STRUVE FUNCTION.
C IS EULERS CONSTANT

```

```

PI=PAI
DMM4=1.

```

```

+PS= .0001
C=0.577215
I=1
J=1
II=1
DUM1=Z/3.0
SUM1=0.0
W=0.0
DJM3=1.0/3.0
EF=0.0
EG=0.0
EH=0.0
EI=0.0
SJM3=0.0
Y=0.0
Q=0.0
P=-0.25*Z
XX=-0.25*Z
SUM4=0.0
SUM5=0.0
DJM6=0.5
SUM7=0.0
DMM3=1.0
SUM9=0.0
CONTINUE
IF(J.EQ.1) GO TO 4
DMM2=DMM2+(1.0/FLOAT(J)+1.0/FLOAT(J+1))
XX=-XX*((0.5*Z)**2)/FLOAT(J*(J+1))
P=-P*((0.5*Z)**2)/FLOAT(J*(J+1))
DUM1=-DUM1*(Z**2)/FLOAT(I*(I+2))
DJM3=-DJM3*(Z**2)/FLOAT(I*(I+2))
DUM6=-DUM6*((0.5*Z)**2)/FLOAT(J*(J+1))
4. DUM2=DUM1*FLOAT(J)
SUM1=SUM1+DUM2
FDH1Z=4.0*SUM1/PI
DUM4=DUM3*FLOAT(I*(I+1))
SUM3=SUM3+DUM4
SDH1Z=SUM3*2.0/PI
DUM7=DUM6*FLOAT(I)
DUM5=DUM6
SUM4=SUM4+DUM5
SUM5=SUM5+DUM7
SUM6=(2.0*((ALOG(0.5*Z)+C)*SUM3+SUM4)+2.0/(Z**2))/PI
SUM7=SUM7+(DUM7*DMM3)/PI
FDY1Z=SUM6+SUM7
Y=Y+XX*0.25*FLOAT((I+1)*(I+2))
Q=Q+P*FLOAT(J)
RR=Q*0.5
SUM8=(2.0*((ALOG(0.5*Z)+C)*Y+SUM5/Z+RR)-4.0/(Z**3))/PI
JJ=J+1
DMM4=DMM4+(1.0/FLOAT(JJ)+1.0/FLOAT(JJ-1))

```



```

      SA=S
      GO TO 1
      IF(JA.GT.1) GO TO 55
      JA=J
      DO 25 J=2,N
      U(J,L)=U(J,L)+T*DS(J)
      CONTINUE
      T=T*.1
      ACCURACY CHECKING
      IF(T.GE.1.0) GO TO 1
      DO 37 IA=2,N
      U(IA,L+1)=U(IA,L)
      CONTINUE
      RETURN
      END

```

```

C
C
C
C *IBFTC SUB4

```

THIS SUBROUTINE CALCULATES THE FUNCTIONAL VALUE

S - FUNCTIONAL VALUE

```

SUBROUTINE FUNVAL(S,U,L)
DIMENSION U(25,21),UBR(25),E(25,25),R(25),X(25)
COMMON/SET1/X,N,NN
COMMON/GRP1/R
COMMON/SET8/UBR,AMEW

```

CALCULATION OF INFLUENCE COEFFICIENT

```

CALL INCOEF(E,U,L)
S=0.0
DO 10 J=2,N
S1=0.0
DO 5 K=2,NN
K1=K+1
S1=S1+E(J,K)*(U(K,L)+U(K1,L))**2/4.
CONTINUE
S=S+(U(J,L)-UBR(J)+AMEW*(-0.5*(U(J,L)**2+0.25*S1)))**2
CONTINUE
RETURN
END

```

```

C
C
C
C *IBFTC SUB5
C

```

THIS SUBROUTINE CALCULATES THE GRADIENT OF FUNCTIONAL VALUE
S W.R.T. VELOCITY

DS - GRADIENT OF THE FUNCTIONAL VALUE

SUBROUTINE GRAD(J,DS,L)
DIMENSION U(25,21),DS(25),YDD(25),I(25,25),X(25),R(25),UBR(25)
COMMON/SET1/X,N,NN
COMMON/GRP1/R
COMMON/SET8/UBR,AMEW

CALCULATION OF INFLUENCE COEFFICIENT

CALL INCOEF(I,U,L)
DO 25 K=2,NN
K1=K+1
DS(K)=0.0
DO 10 I=2,N
S1=0.0
DO 5 J=2,NN
J1=J+1
S1=S1+E(I,J)*(U(J,L)+U(J1,L))**2/4.
CONTINUE
A=2.0*(U(I,L)-UBR(I)+AMEW*(-.5*(U(I,L)**2)+.25*S1))
IF(I.EQ.K) GO TO 15
B=0.25*AMEW*(U(I,K)+U(K1,L))
GO TO 20
15 B=1.0+AMEW*(-U(I,L)+.25*(U(K,K)*(U(K,L)+U(K1,L))))
20 DS(K)=DS(K)+A*B
10 CONTINUE
25 CONTINUE
DS(24)=DS(25)
RETURN
END

*1BFTC SUB6

THIS SUBROUTINE CALCULATES THE LINEAR VELOCITY DISTRIBUTION

SUBROUTINE LINEAR(UBR)
DIMENSION X(25),JBR(25)
COMMON/SET7/YAM,PAI,TC
COMMON/SET1/X,N,NN
PI=PAI
C4=(1.-YAM*YAM)/(2.4*YAM*YAM)

```
1. CONTINUE
   RETURN
   END
```

C
C
C
C
C
C

DATA

[illegible]

0.192	-0.109	-0.165	-0.005	0.182	0.062	0.084	0.092
0.99	0.104	0.106	0.374	0.001	0.02	0.024	0.19
0.12	0.003	0.005	-0.031	-0.065	0.19	-0.151	
0.00	0.005	0.050	0.100	0.20	0.00	0.40	0.5
0.55	0.600	0.620	0.640	0.66	0.68	0.70	0.72
0.7	0.760	0.780	0.800	0.85	0.9	0.95	0.9
0.99	0.11						
0.21	-0.122	-0.073	-0.016	0.127	0.06	0.084	0.092
0.99	0.102	0.105	0.108	0.099	0.041	0.034	0.027
0.18	0.006	-0.006	-0.006	-0.007	-0.012	-0.016	

```

READ 40,AMN,FR,AYAM
MAP=1
T=1./FLOAT(FR)
A=0.5*(1.-SQRT(3.)/3.)
AD=X
ZX=X
EULC=EXP(.577215)
CALL DEVIL(G)
Y(1,1)= 6.*T*T*X*(2.-3.*X)+G
YINI=Y(1,1)
HH= 0.1
TC=T
YAM=AMN
EP=0.001
Z=0.2113249
CC=0.577215
AA=-12.*TC*TC*(1.-2.*Z)
CD=ALOG(2.4*YAM*YAM*TC*Z*(1.-Z)*P(CC))
CE= 12.*TC*TC*(1.-3.*Z)
BB=AA*ALOG(TC*(1.-Z))-CE+AA*CD
P=1.
I=1
30 Q=AA*ALOG(P)+BB
IF(ABS(Q-P)-EP) 1,10,20
20 P=Q
I=I+1
IF(I-1) 1,10,30
10 CONTINUE
Y(1,1)=Y(1,1)+HH*Q
X=X+HH
H=-0.005
U=1.
PRINT 501
PRINT 60,FR,AMN
PRINT 503
PRINT 101,Y(1,1),X
PRINT 505
PRINT 507
PRINT 111
PRINT 507
N=1
CALL FAULAD(N)
100 CONTINUE
STOP
END

```

C
C
C

*IBFTC SUB1

SUBROUTINE FAULAD(N)

358 FORMAT(F6.3)

```

5.7  FORMAT(5X,76(1H*))
3.1  FORMAT(1X,1H*,5(5X,F14.7,5X,1H*),2X,I2)
6    FORMAT(F6.4)
    DIMENSION YP(1,221,5),F(1,221,5),L(1,221,5),YMI(1,221,5),
5Y(1,221,5),FN(1,221,5),CP(221)
    DIMENSION FSUB(1,221),FTRAN(1,221),FSUPER(1,221)
    DIMENSION YIN(1,221),FIN(1,221)
    DIMENSION X1(25),CPL(25)
    COMMON/GRP4/NCAS,NSTAR
    COMMON/PATEL/Q,AYAM
    COMMON/GRP5/XD
    COMMON/GRP6/YINI
    COMMON/SET1/T,AMN,U,PI
    COMMON/SET2/DS2,DS3,DS4,DK,APN,APM,AP,APT
    COMMON/SET5/F
    COMMON/GRP1/K
    COMMON/SET6/X,Y
    COMMON/SET8/YMI
    COMMON/SET9/I
    COMMON/FINK/ZX
    HH= 0.1
    EPS=0.001
    IF(AMN.GE.0.95.AND.AMN.LE.1.25) READ 600,SHK
    MM=1
7    I=1
    CALL REMY(H,N,I)
3.1  JJ=1
5    DO 2 J=1,N
    K=1
    YP(J,I+1,K)=Y(J,I+1,3)+(4./5.)*H*(2.*F(J,I)-F(J,I-1)+2.*F(J,I-2))
    IF(I.EQ.4) E(J,4)=0.
    YMI(J,I+1,K)=YP(J,I+1,K)+(112./121.)*E(J,I)
2    CONTINUE
    J=JJ
    CALL FUNC(FN,J)
    YMI(J,I+1,K+1)=(1./8.)*(9.*Y(J,I)-Y(J,I-2)+3.*H*(FN(J,I+1,K)
5+2.*F(J,I)-F(J,I-1)))
    IF(ABS((YMI(J,I+1,K+1)-YMI(J,I+1,K))/YMI(J,I+1,K+1)).LE.EPS)
5GO TO 15
    IF(K.GE.3) GO TO 30
    K=K+1
    GO TO 40
15.0 E(J,I+1)=(9./121.)*(YMI(J,I+1,K+1)-YMI(J,I+1,1))
    Y(J,I+1)=YMI(J,I+1,K+1)-E(J,I+1)
    JJ=JJ+1
    IF(JJ.LE.N) GO TO 50
    GO TO 35
30    H=H*0.5
    DO 3 J=1,N
3    Y(J,1)=Y(J,I)
    GO TO 70

```

```

15  CONTINUE
    IF(NCAS.NE.2) GO TO 777
    CALL DELTA(FSUB,FTRAN,FSUPER,I)
    IF(NSTAR.EQ.2) GO TO 666
    IF(FSUB(1,I).LE.FTRAN(1,I)) NCAS=1
    NCAS=2
    GO TO 777
666  IF(FSUPER(1,I).LE.FTRAN(1,I)) NCAS=0
    NCAS=2
777  CONTINUE
    IF(NAP.GT.1) GO TO 372
    IF(AMN.EQ.AND.X.GT.SHK) GO TO 123
    GO TO 372
    Y(1,1)=(1.999-AMN*AMN)/(2.4*AMN*AMN)
    X=SHK
    H=0.005
    NAP=3
    NCAS=1
    MM=3
    GO TO 777
372  CONTINUE
    X=X+H
    IF(X.GE.0.97132) GO TO 121
    I=I+1
    CALL VENU(F,I)
    CP(I)=-2.*Y(1,I)/U4.*(T**2)*((1.-2.*X)**2)
    PRINT 506,X,Y(1,I),CP(I),NCAS
    IF(X.GE.0.916.AND.X.LE.1.22) GO TO 55
    MM=MM+1
    IF(MM.GT.2) GO TO 121
    H=-H
    IF(X.GE.1.21) GO TO 121
    HH= HH
    Y(1,1)=YINI+HH*Q
    A=0.2113249+HH
    NSTAR=2
120  CONTINUE
    IF(X.LT.0.97.AND.MM.EQ.2) GO TO 777
    IF(X.LT.0.97.AND.MM.GT.2) GO TO 55
121  CONTINUE
    PRINT 507
    RETURN
    END

```

C
C
C

*IBFTC SUB2

```

SUBROUTINE REMY(H,N,IJ)
500  FORMAT(5X,1H*,3(5X,F14.7,5X,1H*),3X,I2)
    DIMENSION FSUB(1,220),FTRAN(1,220),FSUPER(1,220)
    DIMENSION YA(1,220),PHI(1,220),F(1,220),Y(1,220),Z(1,220)

```

```

DIMENSION CP(22)
COMMON/SET6/X,Y
COMMON/SET1/T,AMN,U,PI
COMMON/GRP4/NCAS,NSTAR
CP(1)=-2.*Y(1,1)/U-4.*(T**2)*((1.-2.*X)**2)
PRINT 500,X,Y(1,1),CP(1),NCAS
DO 80 I=1,3
DO 120 J=1,N
YA(J,I)=Y(J,I)
Z(J,I)=Y(J,I)
120 CONTINUE
CALL VENU(F,I)
DO 130 J=1,N
130 PHI(J,I)=F(J,I)
DO 140 J=1,N
140 Y(J,I)=YA(J,I)+H*.5*F(J,I)
X=X+.5*H
CALL VENU(F,I)
DO 150 J=1,N
150 PHI(J,I)=PHI(J,I)+F(J,I)*2.
DO 160 J=1,N
160 Y(J,I)=YA(J,I)+H*F(J,I)*.5
CALL VENU(F,I)
DO 200 J=1,N
200 PHI(J,I)=(PHI(J,I)+2.*F(J,I))
DO 180 J=1,N
180 Y(J,I)=YA(J,I)+H*F(J,I)
X=X+.5*H
CALL VENU(F,I)
DO 170 J=1,N
170 PHI(J,I)=(PHI(J,I)+F(J,I))*1.6666
DO 180 J=1,N
180 Y(J,I)=YA(J,I)+H*PHI(J,I)
DO 190 J=1,N
Y(J,I+1)=Y(J,I)
Z(J,I+1)=Y(J,I)
190 CONTINUE
IA=I+1
CP(IA)=-2.*Y(1,IA)/U-4.*(T**2)*((1.-2.*X)**2)
PRINT 500,X,Y(1,IA),CP(IA),NCAS
IF(NCAS.NE.2) GO TO 700
CALL DELTA(FSUB,FTRAN,FSUPER,I)
IF(NSTAR.EQ.2) GO TO 600
IF(FSUB(1,I).LE.FTRAN(1,I)) NCAS=1
NCAS=2
GO TO 700
600 IF(FSUPER(1,I).LE.FTRAN(1,I)) NCAS=3
NCAS=2
700 CONTINUE
80 CONTINUE
DO 222 I=1,4

```

```

DD 222 J=1,N
Y(J,I)=I(J,I)
222 CONTINUE
IJ=4
RETURN
END

```

C
C
C

*IBFTC SUB3

```

SUBROUTINE VENU(F,I)
DIMENSION F(1,220),Y(1,220)
COMMON/SET1/T,AMN,U,PI
COMMON/SET2/DS2,DS3,DS4,DK,APN,APM,AP,APT
COMMON/SET6/X,Y
COMMON/GRP4/NCAS,NSTAR
COMMON/GRP2/DS,DS1,AS2,AS3,RX
COMMON/GRP3/EULC,G
COMMON/FINK/ZX
ZX=X
IF(NCAS.EQ.2) GO TO 10
IF(NCAS.EQ.1) GO TO 20
CALL RAJEEV(I)
F(1,I)=U*((DS3*APM*0.25/PI)+(DS2*0.5*APT/PI-(DS2*0.5)/(PI*(1.-X)))-
124.*(T**2)+72.*(T**2)*E)
GO TO 3
1 CALL KUMAR(I)
CALL DEVIL(G)
F(1,1)=(DS1*AS2)/(4.*PI*DS)+(2./((2.4*AMN*AMN*RX*EULC)))*
5 KP((4.*PI)*((Y(1,I)+G*0.5*(AS2*ALOG(T*(1.-X)))/(2.*PI)-
312.*T*T*X*(2.-3.*X)))/AS2))
GO TO 3
2 CALL GAMA(I)
F(1,1)=D*(DB3*0.25*APT/PI+DS3*0.25*APT/PI
5 +DS2*0.25*(1.-2.*X)/(PI*X*(1.-X)))
3 CONTINUE
RETURN
END

```

C
C
C

*IBFTC SUB4

```

SUBROUTINE RAJEEV(I)
DIMENSION Y(1,220)
COMMON/SET1/T,AMN,U,PI
COMMON/SET2/DS2,DS3,DS4,DK,APN,APM,AP,APT
COMMON/SET6/X,Y

```

```

APN=((AMN**2)+DK*Y(1,I)-1.)
APN=ABS(APN)
APM=ALOG(APN)
APT=ALOG(T*(1.-X))
AP=0.0
RETURN
END

```

```

C
C
C
*1BFTC SUB5
SUBROUTINE KUMAR(I)
DIMENSION Y(1,22)
COMMON/GRP2/DS,DS1,AS2,AS3,RX
COMMON/GRP3/EULC,G
COMMON/SET1/T,AMN,U,PI
COMMON/SET6/X,Y
DS=4.*PI*T*T*((X-X**2)**2)
DS1=8.*PI*T*T*(X-2.*X**2+2.*X**3)
AS2=8.*PI*T*T*(1.-6.*X+6.*X**2)
AS3=8.*PI*T*T*(1.-6.*X+12.*X**2)
RX=2.*T*(X-X**2)
RETURN
END

```

```

C
C
C
*1BFTC SUB6
SUBROUTINE GAMA(I)
DIMENSION Y(1,22)
COMMON/SET1/T,AMN,U,PI
COMMON/SET2/DS2,DS3,DS4,DK,APN,APM,AP,APT
COMMON/SET6/X,Y
DS2=8.*PI*(T**2)*(1.-6.*X+6.*X**2)
DS3=8.*PI*(T**2)*(1.-6.*X+12.*X**2)
DS4=96.*PI*(T**2)
DK=2.4*(AMN**2)/J
APN=(1.-AMN**2)+DK*Y(1,I)
APN=ABS(APN)
APM=ALOG(APN)
AP=0.0
APT=ALOG((T**2)*(X-X**2))
RETURN
END

```

```

C
C
C
*1BFTC SUB7
SUBROUTINE FUNC(FN,J)
DIMENSION YMI(1,22,5),Y(1,22,5),FN(1,22,5)
COMMON/GRP1/K

```

```

COMMON/GRP4/NCAS, NSTAR
COMMON/GRP2/DS, DS1, AS2, AS3, RX
COMMON/GRP3/FULC, G
COMMON/SET9/I
COMMON/SET1/T, AMN, U, PI
COMMON/SET11/DS2, DS3, DS4, DK, APN, APM, APT
COMMON/SET5/H
COMMON/SET6/Z, Y
COMMON/SET8/YMI
COMMON/FINK/ZX
X=Z+H
ZX=X
IF(NCAS.EQ.2) GO TO 10
IF(NCAS.EQ.1) GO TO 20
CALL SIDDU(I)
FN(1,I+1,K)=U*((DS3*APM*.25/PI)+DS3*.5*APT/PI
5(DS2*.5)/(PI*(1.-X))-24.*(T**2)+72.*(T**2)*X)
GO TO 3
1 CALL FISH(I)
CALL DEVIL(G)
FN(1,I+1,K)=(DS1*AS3)/(4.*PI*DS)+(2./(2.4*AMN*AMN*RX*FULC))*
5EXP((4.*PI)*((YMI(1,I+1,K)+G*.5*(AS2*ALOG(T*(1.-X)))/(2.*PI)-
512.*T*T*X*(2.-3.*X)))/AS2))
GO TO 3
2 CALL NEWTON(I)
FN(1,I+1,K)=U*(DS3*.25*APM/PI+.75*DS3/PI+DS3*.25*APT/PI
5+DS2*.25*(1.-2.*X)/(PI*X*(1.-X)))
CONTINU
RETURN
END

```

C
C
C

*IBFTC SUB8

```

SUBROUTINE SIDDU(I)
DIMENSION YMI(1,22,5),Y(1,22)
COMMON/SET5/H
COMMON/GRP1/K
COMMON/SET10/DS2, DS3, DS4, DK, APN, APM, APT
COMMON/SET11/T, AMN, U, PI
COMMON/SET6/Z, Y
COMMON/SET8/YMI
X=Z+H
DS2=8.*PI*(T**2)*(1.-6.*X+6.*(T**2))
DS3=8.*PI*(T**2)*(-6.+12.*X)
DS4=96.*PI*(T**2)
DK=(AMN**2)*2.4/U
APN=((AMN**2)+DK*YMI(1,I+1,K)+1.)
APN=ABS(APN)
APM=ALOG(APN)
APT=ALOG(T*(1.-X))

```


RETURN
END

C
C
C

*1BFTC SUB9

```
SUBROUTINE NEWTON(I)
DIMENSION YMI(1,220,5)=Y(1,220)
COMMON/GRP1/K
COMMON/SET10/DS2,DS3,DS4,DK,APN,APM,AFT
COMMON/SET1/T,AMN,U,PI
COMMON/SET5/H
COMMON/SET6/Z,Y
COMMON/SET8/YMI
X=Z+H
DS2=8.*PI*(T**2)*(1.-6.*X+6.*(X**2))
DS3=8.*PI*(T**2)*(1.-6.+12.*X)
DS4=96.*PI*(T**2)
DK=2.4*(AMN**2)/U
APN=(1.-(AMN**2)+DK*YMI(1,I+1,K))
APN=ABS(APN)
APT=ALOG((T**2)*(X-(X**2)))
APM=ALOG(APN)
RETURN
END
```

C
C
C

*1BFTC SUB10

```
SUBROUTINE DELTA(FSUB,FTRAN,FSUPER,I)
DIMENSION FSUB(1,220),FTRAN(1,220),FSUPER(1,220),Y(1,220)
COMMON/SET1/T,AMN,U,PI
COMMON/SET6/X,Y
COMMON/GRP4/NCAS,NSTAR
COMMON/SET2/DS2,DS3,DS4,DK,APN,APM,AP,APT
COMMON/GRP2/DS,DS1,AS2,AS3,RX
COMMON/GRP3/EULC,G
COMMON/FINK/ZX
ZX=X
IF(NCAS.NE.2) GO TO 200
IF(NCAS.EQ.2.AND.NSTAR.EQ.1) GO TO 100
CALL RAJEEV(I)
FSUPER(1,I)=U*((DS3*APM*0.25/PI)+DS3*0.5*APT/PI-(DS2*0.5)/(PI*
5(1.-X))-24.*(T**2)+72.*(T**2)*X)
100 CONTINUE
CALL KUMAR(I)
CALL DEVIL(G)
FTRAN(1,I)=(DS1*AS3)/(4.*PI*DS)+(2./(2.4*AMN*AMN*RX*EULC))*
EXP((4.*PI)*((Y(1,I)+G-0.5*(AS2*ALOG(T*(1.-X)))/(2.*PI)-
512.*T*T*X*(2.-3.*X)))/AS2))
IF(NCAS.EQ.2.AND.NSTAR.EQ.2) GO TO 200
```

```

CONTINU
CALL GAMA(I)
FSUB(1,I)=U*(DS3*.25*APM/PI+.25*DS3/PI+DS3*.25*APT/PI
+DS2*0.25*(1.-2.*X)/(PI*(1.-X)))
CONTINU
RETURN
END

```

C
C
C
*IBFTC SUB11

```

SUBROUTINE FISH(I)
DIMENSION YMI(1,22),E)
DIMENSION Y(1,22)
COMMON/GRP2/DS,DS1,AS2,AS3,R
COMMON/GRP3/EULC,G
COMMON/SET8/YMI
COMMON/SET1/T,AMN,U,PI
COMMON/SET5/F
COMMON/SET6/Z,Y
X=Z+H
DS=4.*PI*T*T*(X-X*X)**2)
DS1=8.*PI*T*T*(X-3.*X*X+2.*X*X*X)
AS2=8.*PI*T*T*(1.-6.*X+6.*X*X)
AS3=8.*PI*T*T*(-5.+12.*X)
RX=2.*T*(X-X*X)
RETURN
END

```

C
C
C
*IBFTC SUB12

```

SUBROUTINE DEVIL(G)
COMMON/SET11/T,AMN,U,PI
COMMON/FINK/ZX
X=ZX
ZETA=(AMN*AMN-1.)/(2.4*AMN*AMN*T*T)
IF(AMN.LT.1.0) G=-6.*T*T*X*(2.-3.*X)*(1.-EXP(-ZETA/(-6.*X*
5(2.-3.*X))))
IF(AMN.GT.1.0) G=6.*T*T*X*(2.-3.*X)*(1.-EXP(ZETA/(-6.*X*
5(2.-3.*X))))
RETURN
END

```

*ENTRY

C
C
C
C
C
C
DATA CARDS
11

1.0 100.000
1.9 100.000
1.95 100.950
1.9452
1.975 100.975
1.6690
1.99 100.990
1.7148
1.0101 1.010
1.7982
1.0251 1.025
1.8831
1.0501 1.050
1.0751 1.075
1.10 101.000
1.20 101.000